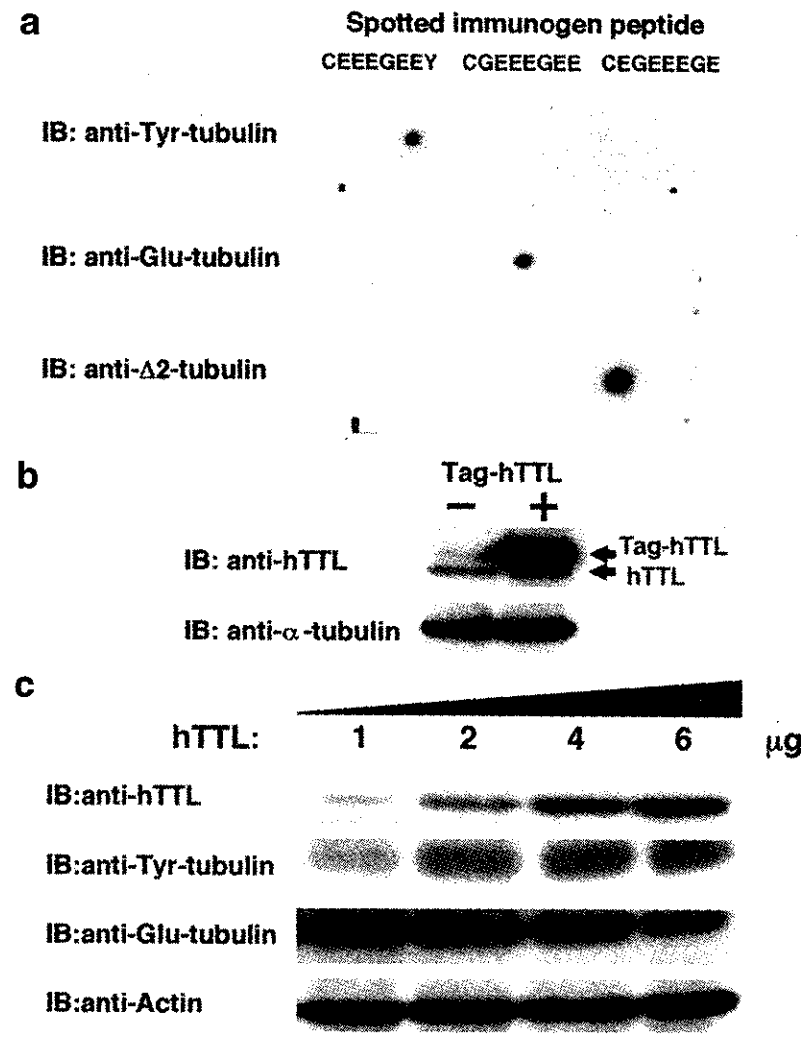

FIGURE 3 – hTTL has a tyrosination activity in mammalian cultured cells. (*a*) Specificity of antibodies. The indicated synthetic peptides were spotted on the filter and immunoblotted with the polyclonal anti-Tyr-tubulin (top), anti-Glu-tubulin (middle), or anti-Δ2-tubulin antibody (bottom). (*b*) Expression of FLAG-tagged hTTL. Whole-cell lysates prepared from COS7 cells transfected with the empty plasmid or with the expression plasmid for FLAG-tagged hTTL were subjected to immunoblotting with the anti-hTTL antibody (top). The expression level of α-tubulin was examined to ensure equal loading (bottom). (*c*) The exogenously expressed hTTL has a catalytic activity. HEK293T cells were transfected with increasing amounts of the hTTL expression plasmid. Forty-eight hours after transfection, whole-cell lysates were prepared and immunoblotted with the indicated antibodies. The expression level of actin is included as a loading control (bottom).

cells with 1 nM BMP2 or 5 μM RA induced remarkable morphologic differentiation by day 8. The hTTL protein level was increased after day 2 and peaked on day 6 in the former and on day 3 in the latter. Thereafter, it appeared to be decreased. Thus, hTTL was induced during induction of neuronal differentiation in NBL cells.

Expression of hTTL mRNA in primary neuroblastomas

To evaluate the clinical significance of *hTTL*, we examined the expression of *hTTL* mRNA in 16 favorable (stage 1, high expression of *TrkA* and a single copy of *MYCN*) and 16 unfavorable (stage 3 or 4, low expression of *TrkA* and amplification of *MYCN*) NBLs using semiquantitative RT-PCR. As shown in Figure 5(*a*), *hTTL* was preferentially expressed in favorable NBLs. Therefore, we next performed quantitative real-time RT-PCR to measure the levels of *hTTL* transcript in 74 primary NBLs. Table I shows the quantitative levels of *hTTL* mRNA expression (mean ± SEM) by age (< 1-year-old *vs.* ≥ 1-year-old), tumor stages (1 + 2 + 4s *vs.* 3 + 4), *TrkA* expression (low *vs.* high), *MYCN* gene copies (single *vs.* amplified), origin (adrenal gland *vs.* others), mass screening (tumors found by mass screening *vs.* sporadic tumors) and prognosis (alive *vs.* dead). High levels of *hTTL* expression were significantly associated with favorable stages ($p = 0.0069$), high *TrkA* expression ($p = 0.002$), a single copy of *MYCN* ($p < 0.00005$), tumors found by mass screening ($p = 0.0042$), origins other than adrenal gland ($p = 0.0042$) and a good prognosis ($p = 0.023$). *hTTL* expression was marginally associated with age. The log-rank test indicated that *hTTL* expression was associated with better survival ($p = 0.026$), which was also indicated in the Kaplan-Meier cumulative survival curves (Fig. 5*b*).

The univariate Cox regression was employed to examine the individual relationship of each variable to survival (Table II). Expression of *hTTL*, age, *MYCN* copy numbers and mass screening were found to be of prognostic importance, supporting the results of the log-rank test. However, since *hTTL* expression was highly associated with *MYCN*, mass screening and origin, multivariable Cox models were not fitted to assess the predictive importance of *hTTL* expression for survival after controlling these prognostic factors, suggesting that expression of *hTTL* was not an independent prognostic indicator.

FIGURE 2 – Genomic structure, alignment of amino acid sequence and mRNA expression of human *TTL*. (*a*) Genomic structure of *hTTL*. The *hTTL* gene that is mapped to 2q13 consists of 7 exons. Untranslated regions (open boxes) and coding regions (hatched boxes) are shown. Numbers indicate nucleotide position in human BAC clone *RP11-1I24* (accession number AC012442). (*b*) Comparison of amino acid sequences among mammalian TTLs. The gaps produced by the alignment are indicated by a hyphen in the sequence. The conserved amino acid residues in TTLs are shown by asterisks below the alignment. (*c*) Tissue distribution of *hTTL* mRNA. The expression levels of *hTTL* mRNA in the indicated human tissues were examined by semiquantitative RT-PCR (top). *GAPDH* expression was also examined as an internal control (bottom).

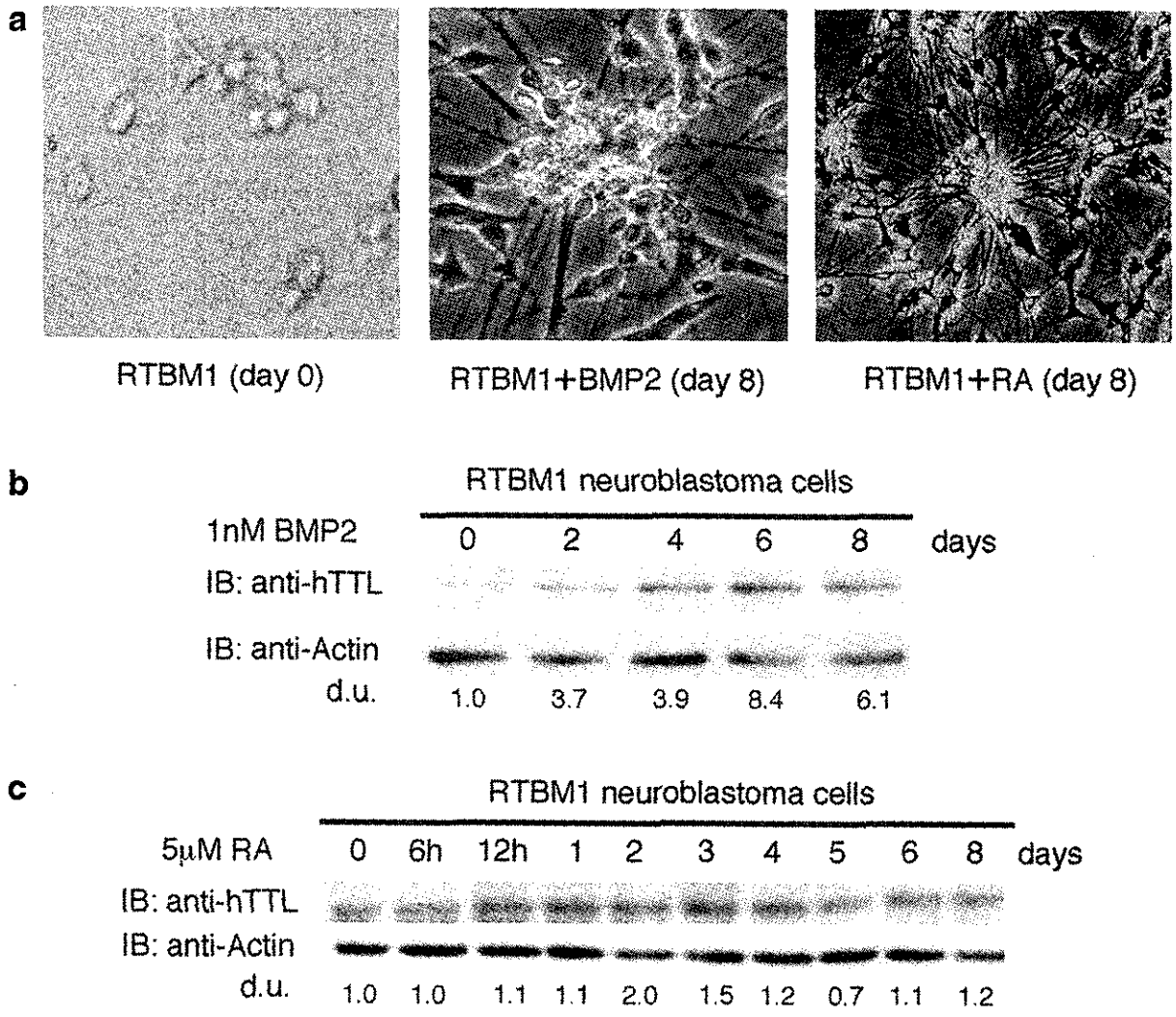

FIGURE 4 – TTL is induced during BMP2- and RA-mediated neuroblastoma differentiation. (*a*) BMP2- or RA-induced morphologic changes in RTBM1 neuroblastoma cells. RTBM1 cells were treated with BMP2 or RA at a final concentration of 1 nM or 5 μM, respectively, and maintained for 8 days. (*b*) Expression levels of hTTL are increased in response to BMP2. At the indicated time points after the treatment with BMP2 (at a final concentration of 1 nM), whole-cell lysates prepared from RTBM1 cells were subjected to immunoblotting with the antibody against hTTL (top). Actin protein levels were determined as a loading control (bottom). (*c*) Induction of hTTL in response to RA. RTBM1 cells were exposed to RA at a final concentration of 5 μM. Whole-cell lysates were prepared at the indicated time points after the treatment with RA and subjected to immunoblotting with the anti-hTTL (top) or with antiactin (bottom) antibody. d.u., arbitrary density units.

Immunohistochemistry

To determine the expression pattern of hTTL protein in primary NBLs, we performed immunohistochemical study for 6 favorable (stage 1 or 2 and a single copy of *MYCN*) and 4 unfavorable (stage 3 or 4 and amplified *MYCN*) NBLs. hTTL, Tyr-tubulin and Glu-tubulin were positively detected both in the cytoplasm of the neuroblastic cells and in the fine meshwork of neuropil of all 6 tumors with favorable histology (Shimada's classification) and a single copy of *MYCN* (Fig. 6*a–c*). In contrast, all 4 tumors with unfavorable histology and *MYCN* amplification were negative for Tyr-tubulin and Glu-tubulin, and only 1 tumor in this subset was positive for hTTL (Fig. 6*f–h*). Interestingly, all 10 NBL tumors were positive for Δ2-tubulin, but whose staining pattern was rather distinct in different subsets of the tumors. In the favorable tumors, Δ2-tubulin showed a localization similar to hTTL, Tyr-tubulin and Glu-tubulin and was detected in the cytoplasm and in the fine neuropil (Fig. 6*d*). On the other hand, Δ2-tubulin in the aggressive tumors was found only in the cytoplasm of neuroblastic cells, since they had no or a very limited capability of neuritic process production (*i.e.*, neuropil formation; Fig. 6*i*).

CD56 was detected in all 10 tumors, regardless of the histology and *MYCN* status (data not shown). TrkA was detected in all of 6 favorable tumors (Fig. 6*e*), but was negative in 3 of 4 aggressive tumors (Fig. 6*j*). It was noted that one unfavorable tumor with weakly positive trkA showed positive staining for TTL. Ki-67 staining revealed 10–20% and 60–70% positive cells in the favorable and the unfavorable tumors, respectively (data not shown).

DISCUSSION

In the present study, we have identified human ortholog of *tubulin tyrosine ligase* gene, which is highly conserved among the mammalian species. *hTTL* mRNA is ubiquitously expressed but rather preferential in both fetal and adult brains as well as in lung. The specific antibodies raised against hTTL, Tyr-tubulin, Glu-tubulin and Δ2-tubulin have confirmed the catalytic activity of

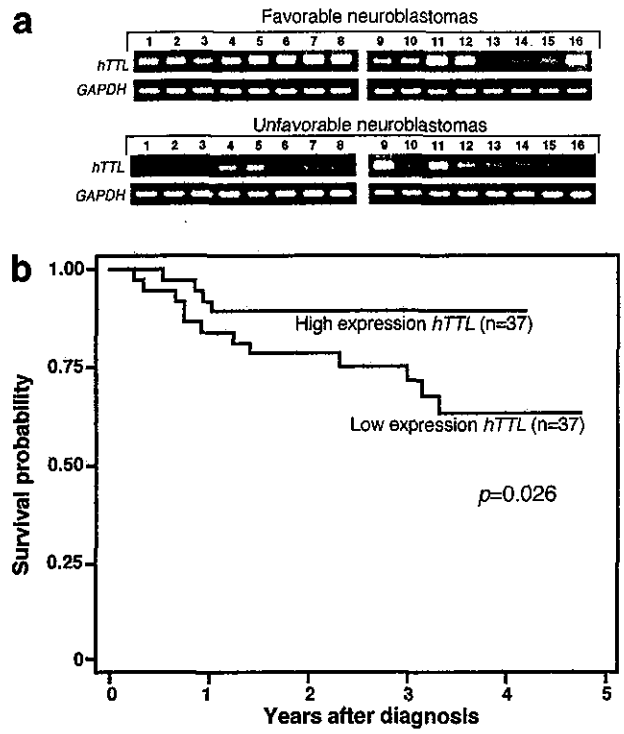

FIGURE 5 – Expression of *hTTL* mRNA is associated with unfavorable prognosis of neuroblastoma. (*a*) Total RNA was purified from the indicated favorable (top) and unfavorable NBL tissues (bottom) and subjected to semiquantitative RT-PCR. Sixteen favorable cases used in this study were classified as stage 1 NBL with a single copy *MYCN* as well as a high expression of *TrkA*. Sixteen unfavorable cases were in stages 3 and 4 NBL with *MYCN* amplification as well as a low *TrkA* expression. *GAPDH* expression was also examined as an internal control. (*b*) Association of *hTTL* mRNA expression levels with favorable prognosis of NBL. Total RNA was prepared from 74 NBL tissues, and *hTTL* mRNA levels were assayed by quantitative real-time RT-PCR as described in text. The values of *hTTL* mRNA were normalized by *GAPDH*. The survival of *hTTL* relatively high-expression group (n = 37) and *hTTL* low-expression group (n = 37) was compared using the Kaplan-Meier procedure.

TABLE I – RESULTS OF LOG-RANK TESTS FOR CONVENTIONAL PROGNOSTIC FACTORS AND EXPRESSION OF *hTTL* IN 74 PRIMARY NEUROBLASTOMAS

Variable	n	*hTTL* expression[1]	p-value
Age (year)			0.1
<1	43	117 ± 14	
≥ 1	31	77 ± 10	
Tumor stage			0.0069
1, 2, 4s	40	127 ± 14	
3, 4	34	69 ± 9	
TrkA expression			0.002
High	36	125 ± 17	
Low	38	77 ± 8	
MYCN			<0.00005
Single	52	123 ± 11	
Amplified	22	46 ± 9	
Mass screening			0.0042
+	37	128 ± 14	
−	37	72 ± 10	
Origin			0.0042
Adrenal gland	47	85 ± 11	
Others	27	127 ± 16	
Prognosis			0.023
Alive	58	113 ± 11	
Dead	16	54 ± 11	

[1]Mean ± SEM.

TABLE II – COX REGRESSION MODELS USING DICHOTOMOUS FACTORS OF AGE, *MYCN* AMPLIFICATION, MASS SCREENING, ORIGIN AND EXPRESSION OF *hTTL*

Factor	p-value	Hazard ratio (95% confidence interval)
hTTL expression (log)	0.024	0.64 (0.44, 0.94)
Age (> 1 *vs.* < 1 year)	0.005	5.04 (1.61, 15.8)
MYCN (1 copy *vs.* > 1 copy)	<0.0005	0.06 (0.017, 0.22)
Mass screening (+ *vs.* −)	0.004	0.05 (0.007, 0.38)
Origin (adrenal gland *vs.* others)	0.31	1.79 (0.58, 5.57)

hTTL encoded by the *hTTL* gene in the cells. Interestingly, hTTL is induced during neurite extension in RTBM1 NBL cells treated with BMP2 or RA, suggesting that hTTL expression is associated with neuronal differentiation in human NBL. Immunohistochemically, favorable NBLs are positive for hTTL, Tyr-tubulin, Glu-tubulin and Δ2-tubulin, whereas unfavorable tumors with *MYCN* amplification are positive only for Δ2-tubulin, suggesting that deregulation of tyrosination/detyrosination cycle contributes to malignant progression of NBL. This hypothesis has been further supported by a significant decrease of the levels of *hTTL* expression in the patients with poor prognosis.

The dynamics of microtubule regulates many cellular functions, including migration, motility, differentiation, cell division and cellular cap formation. Though posttranslational modifications of tubulin and their enzymatic regulation have long been studied, the precise mechanisms are still largely unknown. It is interesting that no orthologs of highly conserved mammalian TTL have so far been reported in *Caenorhabditis elegans*, *Drosophila melanogaster* and *Saccharomyces cerevisiae*, suggesting that the tyrosination/detyrosination cycle of tubulin may be related to evolution of the cellular functions, including neuronal differentiation. In newborn rats, TTL expression is found in skeletal muscle at high levels and is developmentally regulated by rapidly decreasing its level during early postnatal period.[31] It is interesting that both BMP2 and RA, which have increased levels of hTTL expression, function as regulators to induce differentiation during neural development.

The tyrosination/detyrosination of tubulin may be regulated by the activities of both TTL and tubulin carboxypeptidase (TCP). Until now, however, the *TCP* gene has never been identified in vertebrates, although biochemical TCP activity has been reported to be present in some subcellular fractions.[18] Tubulin is also posttranslationally modified by nitrotyrosination. Eiserich *et al.*[32] showed that free 3-nitrotyrosine (NO_2Tyr) is transported into mammalian cells and selectively incorporated into the Glu-tubulin posttranslationally, which is catalyzed by TTL. Cellular injury such as microtubule disorganization has consequently been induced. Kalisz *et al.*[33] also showed that nitrotyrosine can be incorporated into α-tubulin by *in vitro* assays. Those reports demonstrated that carboxypeptidase A is incapable of cleaving nitrotyrosine from the modified α-tubulin. On the other hand, Bisig *et al.*[34] reported that nitrotyrosinated tubulin is a good substrate of physiologic TCP, and that it has a similar capability to that of the tyrosinated tubulin to assemble into microtubules, suggesting that incorporation of nitrotyrosine is not injurious at least to dividing cells. Therefore, whether nitrotyrosinated tubulin is harmful or not is still controversial. Nevertheless, as increased nitrotyrosination is reported in Alzheimer's disease and amyotrophic lateral sclerosis,[35–37] the functional analysis of the role of hTTL and tubulin tyrosination/detyrosination cycle should be important for understanding the pathogenesis of these disease. The treatment of cells with methylmercury (MeHg) is also reported to induce perturbation of cellular activities associated with the tubulin/microtubule system by altering the status of tubulin tyrosination in the rat

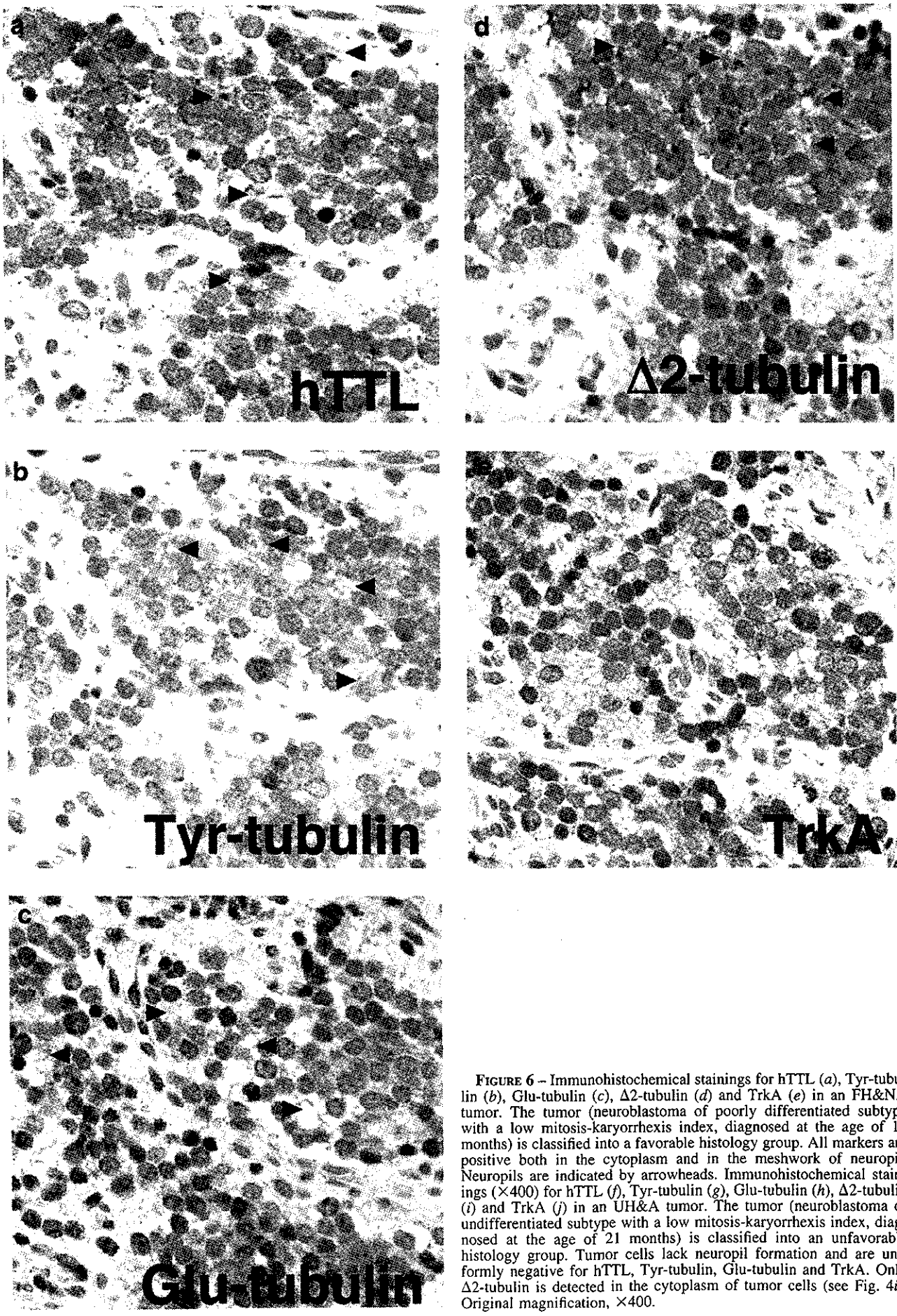

FIGURE 6 – Immunohistochemical stainings for hTTL (*a*), Tyr-tubulin (*b*), Glu-tubulin (*c*), Δ2-tubulin (*d*) and TrkA (*e*) in an FH&NA tumor. The tumor (neuroblastoma of poorly differentiated subtype with a low mitosis-karyorrhexis index, diagnosed at the age of 10 months) is classified into a favorable histology group. All markers are positive both in the cytoplasm and in the meshwork of neuropil. Neuropils are indicated by arrowheads. Immunohistochemical stainings (×400) for hTTL (*f*), Tyr-tubulin (*g*), Glu-tubulin (*h*), Δ2-tubulin (*i*) and TrkA (*j*) in an UH&A tumor. The tumor (neuroblastoma of undifferentiated subtype with a low mitosis-karyorrhexis index, diagnosed at the age of 21 months) is classified into an unfavorable histology group. Tumor cells lack neuropil formation and are uniformly negative for hTTL, Tyr-tubulin, Glu-tubulin and TrkA. Only Δ2-tubulin is detected in the cytoplasm of tumor cells (see Fig. 4*i*). Original magnification, ×400.

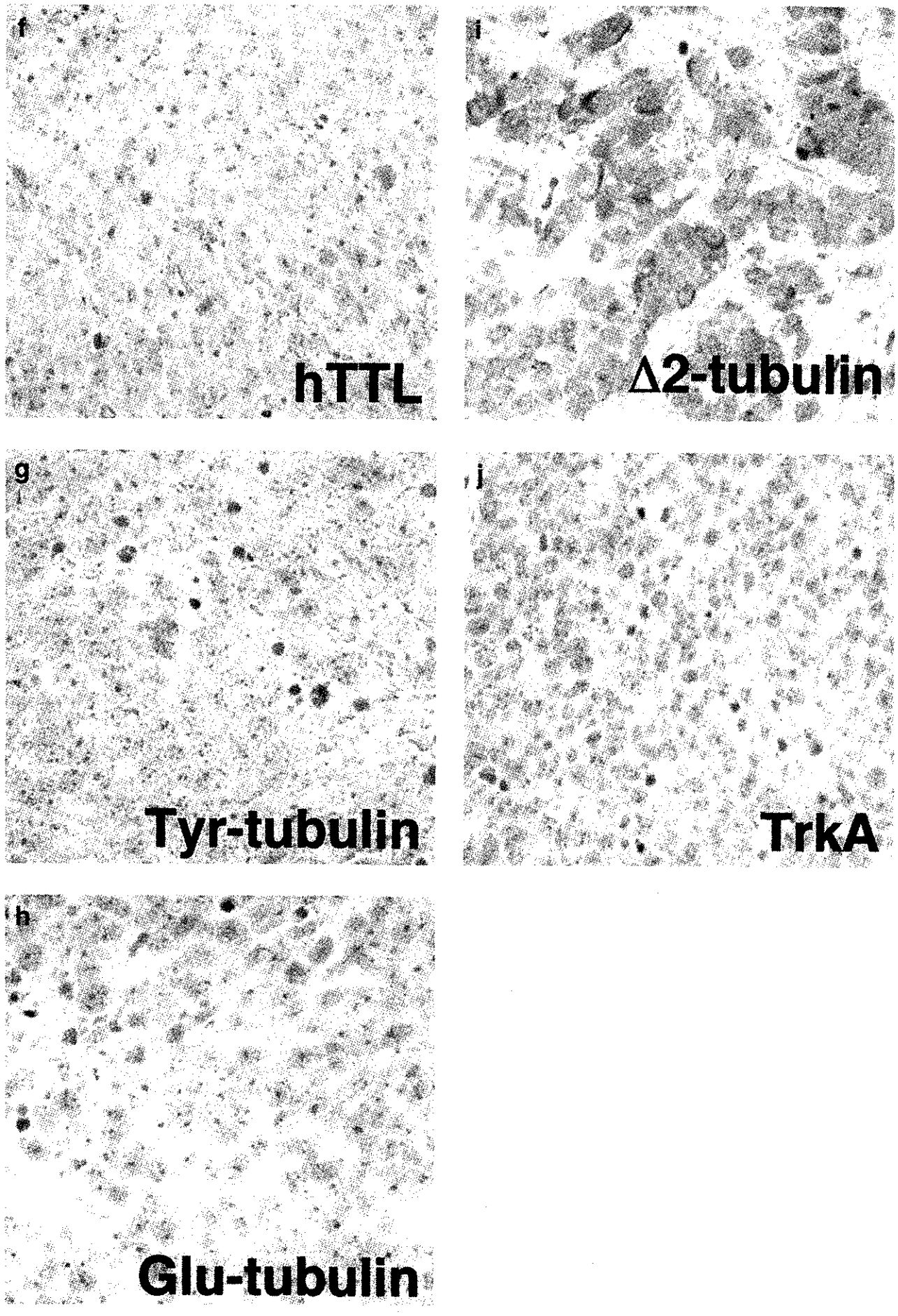

FIGURE 6 – (CONTINUED)

brain.[38] Therefore, many cellular stresses such as oxidative damage may trigger dysfunction of the tubulin/microtubule cytoskeletal system.

Our present study has shown that the decreases in Tyr-tubulin and Glu-tubulin are associated with relatively low levels of hTTL expression in unfavorable NBLs, which have lost a potency of neuronal differentiation and/or apoptosis. They are also correlated with decreased levels of TrkA, a high-affinity receptor for nerve growth factor, whose activation induces morphologic differentiation of NBL cells.[39] In addition, gradual upregulation of hTTL has been observed during induction of neuronal differentiation in RTBM1 cells treated with BMP2 or RA. These suggest that the induction of neuronal differentiation in NBL is accompanied with the activated tyrosination/detyrosination cycle regulated by increased level of hTTL enzyme, while the cycle is arrested by downregulation of hTTL in proliferating NBL cells, resulting in accumulation of Δ2-tubulin within the cells. Indeed, the expression levels of *hTTL* mRNA and Δ2-tubulin are significantly correlated with the prognosis of primary NBLs. This is consistent with the observation that TTL activity is lost, and conversely Δ2-tubulin is upregulated during the tumor cell growth.[19] Lafanechere *et al.*[19] have demonstrated by using mouse TTL null cells both *in vitro* and *in vivo* that mouse TTL activity is strongly decreased during tumor growth. Mas *et al.*[15] have also reported that, using rat *TTL* dominant negative mutant and an antisense cDNA of rat *TTL*, suppression of TTL activity induces 2- to 3-fold faster cell proliferation. Moreover, in human breast cancers, the accumulation of Glu-tubulin and Δ2-tubulin is correlated with poor prognosis by immunohistochemical approach.[28] It is noteworthy that our preliminary data using the microarray hybridized with total RNA obtained from 136 primary NBLs have shown that the gene with the highest score to predict prognosis of NBLs is α-tubulin (data not shown). Thus, the role of microtubule and its component, α-tubulin, is very important to define the biology as well as the aggressiveness of cancer cells.

In conclusion, we have identified a *human tubulin tyrosine ligase* gene and demonstrated its tissue distribution and correlation with neuronal differentiation. Since our data have suggested that the tyrosination cycle of α-tubulin is activated in differentiating NBLs but is inactivated in proliferating tumors, the cycle-related molecules including hTTL could be the targets for developing novel therapeutic strategies against advanced stages of NBL.

ACKNOWLEDGEMENTS

The authors thank Shigeru Sakiyama for critical reading of the manuscript, Naoko Sugimitsu for preparing RNA, Yuki Nakamura for DNA sequencing, Yoshiaki Okamoto for instructing quantitative real-time RT-PCR and Aiko Morohashi and Natsue Akao for technical assistance. The authors also thank the following institutions for providing surgical samples: First Department of Surgery, Hokkaido University School of Medicine; Department of Pediatrics, National Sapporo Hospital; Department of Pediatric Surgery, Tohoku University School of Medicine; Department of Surgery, Gunma Children's Medical Center; Department of Pediatrics, Pediatric Surgery and General Surgery, Jichi Medical University; Department of Hematology and Oncology, Saitama Children's Medical Center; Department of Pediatrics, Juntendo University School of Medicine; Department of Surgery, Kiyose Metropolitan Children's Hospital; Department of Surgery and Pathology, Chiba Children's Hospital; Department of Pediatric Surgery, Chiba University School of Medicine; Department of Pediatric Surgery, Kimitsu Central Hospital; Department of Pediatric Surgery, Niigata University School of Medicine; Department of Pediatrics and Pediatric Surgery, Aichi Medical University; Department of Pediatrics, Kyoto Prefectural Medical University; Tumor Board, Hyogo Children's Hospital; Department of Pediatrics and Pediatric Surgery, Kagoshima University School of Medicine; Department of Pediatric Surgery, Showa University School of Medicine; Department of Pediatrics, Oita University School of Medicine; Department of Pediatric Surgery, Ohta General Hospital; Department of Pediatrics, Ichinomiya City Hospital; Department of Pediatric Surgery, Osaka City General Hospital; Department of Pediatrics, Nihon University School of Medicine; Itabashi Hospital; Department of Pediatric Surgery, University of Tsukuba School of Medicine.

REFERENCES

1. MacRae TH. Tubulin post-translational modifications: enzymes and their mechanisms of action. Eur J Biochem 1997;244:265–78.
2. Zambito AM, Wolff J. Palmitoylation of tubulin. Biochem Biophys Res Commun 1997;239:650–4.
3. Barra HS, Arce CA, Argarana CE. Posttranslational tyrosination/detyrosination of tubulin. Mol Neurobiol 1988;2:133–53.
4. Luduena RF. Multiple forms of tubulin: different gene products and covalent modifications. Int Rev Cytol 1998;178:207–75.
5. Barra HS, Unates LE, Sayavedra MS, Caputto R. Capacities for binding amino acids by tRNAs from rat brain and their changes during development. J Neurochem 1972;19:2289–97.
6. Barra HS, Rodriguez JA, Arce CA, Caputto R. A soluble preparation from rat brain that incorporates into its own proteins (14 C)arginine by a ribonuclease-sensitive system and (14 C)tyrosine by a ribonuclease-insensitive system. J Neurochem 1973;20:97–108.
7. Barra HS, Arce CA, Rodriguez JA, Caputto R. Incorporation of phenylalanine as a single unit into rat brain protein: reciprocal inhibition by phenylalanine and tyrosine of their respective incorporations. J Neurochem 1973;21:1241–51.
8. Barra HS, Arce CA, Rodriguez JA, Caputto R. Some common properties of the protein that incorporates tyrosine as a single unit and the microtubule proteins. Biochem Biophys Res Commun 1974;60:1384–90.
9. Arce CA, Rodriguez JA, Barra HS, Caputo R. Incorporation of L-tyrosine, L-phenylalanine and L-3,4-dihydroxyphenylalanine as single units into rat brain tubulin. Eur J Biochem 1975;59:145–9.
10. Argarana CE, Arce CA, Barra HS, Caputto R. *In vivo* incorporation of [14C]tyrosine into the C-terminal position of the alpha subunit of tubulin. Arch Biochem Biophys 1977;180:264–8.
11. Preston SF, Deanin GG, Hanson RK, Gordon MW. The phylogenetic distribution of tubulin:tyrosine ligase. J Mol Evol 1979;13:233–44.
12. Gabius HJ, Graupner G, Cramer F. Activity patterns of aminoacyl-tRNA synthetases, tRNA methylases, arginyltransferase and tubulin: tyrosine ligase during development and ageing of *Caenorhabditis elegans*. Eur J Biochem 1983;131:231–4.
13. Stieger J, Wyler T, Seebeck T. Partial purification and characterization of microtubular protein from *Trypanosoma brucei*. J Biol Chem 1984;259:4596–602.
14. Ersfeld K, Wehland J, Plessmann U, Dodemont H, Gerke V, Weber K. Characterization of the tubulin-tyrosine ligase. J Cell Biol 1993;120:725–32.
15. Mas CR, Arregui CO, Filiberti A, Argarana CE, Barra HS. Cloning of rat olfactory bulb tubulin tyrosine ligase cDNA: a dominant negative mutant and an antisense cDNA increase the proliferation rate of cells in culture. Neurochem Res 2002;27:1453–8.
16. Paturle-Lafanechere L, Edde B, Denoulet P, Van Dorsselaer A, Mazarguil H, Le Caer JP, Wehland J, Job D. Characterization of a major brain tubulin variant which cannot be tyrosinated. Biochemistry 1991;30:10523–8.
17. Paturle-Lafanechere L, Manier M, Trigault N, Pirollet F, Mazarguil H, Job D. Accumulation of delta 2-tubulin, a major tubulin variant that cannot be tyrosinated, in neuronal tissues and in stable microtubule assemblies. J Cell Sci 1994;107:1529–43.
18. Lafanechere L, Job D. The third tubulin pool. Neurochem Res 2000;25:11–8.
19. Lafanechere L, Courtay-Cahen C, Kawakami T, Jacrot M, Rudiger M, Wehland J, Job D, Margolis RL. Suppression of tubulin tyrosine ligase during tumor growth. J Cell Sci 1998;111:171–81.
20. Ohira M, Morohashi A, Inuzuka H, Shishikura T, Kawamoto T, Kageyama H, Nakamura Y, Isogai E, Takayasu H, Sakiyama S, Suzuki Y, Sugano S, Goto T, Sato S, Nakagawara A. Expression profiling and characterization of 4200 genes cloned from primary neuroblastomas: identification of 305 genes differentially expressed between favorable and unfavorable subsets. Oncogene 2003;22:5525–36.
21. Ohira M, Morohashi A, Nakamura Y, Isogai E, Furuya K, Hamano S, Machida T, Aoyama M, Fukumura M, Miyazaki K, Suzuki Y, Sugano S, Hirato J, Nakagawara A. Neuroblastoma oligo-capping cDNA

project: toward the understanding of the genesis and biology of neuroblastoma. Cancer Lett 2003;197:63–8.
22. Brodeur GM, Pritchard J, Berthold F, Carlsen NL, Castel V, Castelberry RP, De Bernardi B, Evans AE, Favrot M, Hedborg F, kaneko M, Kemshead J, Lampert F, Lee RE, Look AT, Pearson AD, Philip T, Roald B, Sawada T, Seeger RC, Thuchida Y, Voute PA. Revisions of the international criteria for neuroblastoma diagnosis, staging, and response to treatment. J Clin Oncol 1993;11:1466–77.
23. Kaneko M, Nishihira H, Mugishima H, Ohnuma N, Nakada K, Kawa K, Fukuzawa M, Suita S, Sera Y, Tsuchida Y. Stratification of treatment of stage 4 neuroblastoma patients based on N-myc amplification status: Study Group of Japan for Treatment of Advanced Neuroblastoma, Tokyo, Japan. Med Pediatr Oncol 1998;31:1–7.
24. Hishiki T, Nimura Y, Isogai E, Kondo K, Ichimiya S, Nakamura Y, Ozaki T, Sakiyama S, Hirose M, Seki N, Takahashi H, Ohnuma N, Tanabe M, Nakagawara A. Glial cell line-derived neurotrophic factor/neurturin-induced differentiation and its enhancement by retinoic acid in primary human neuroblastomas expressing c-Ret, GFR alpha-1, and GFR alpha-2. Cancer Res 1998;58:2158–65.
25. Chomczynski P, Sacchi N. Single-step method of RNA isolation by acid guanidinium thiocyanate-phenol-chloroform extraction. Anal Biochem 1987;162:156–9.
26. Shimada H, Ambros IM, Dehner LP, Hata J, Joshi VV, Roald B, Stram DO, Gerbing RB, Lukens JN, Matthay KK, Castleberry RP. The International Neuroblastoma Pathology Classification (the Shimada system). Cancer 1999;86:364–72.
27. Goto S, Umehara S, Gerbing RB, Stram DO, Brodeur GM, Seeger RC, Lukens JN, Matthay KK, Shimada H. Histopathology (International Neuroblastoma Pathology Classification) and MYCN status in patients with peripheral neuroblastic tumors: a report from the Children's Cancer Group. Cancer 2001;92:2699–708.
28. Mialhe A, Lafanechere L, Treilleux I, Peloux N, Dumontet C, Bremond A, Panh MH, Payan R, Wehland J, Margolis RL, Job D. Tubulin detyrosination is a frequent occurrence in breast cancers of poor prognosis. Cancer Res 2001;61:5024–7.
29. Iwasaki S, Hattori A, Sato M, Tsujimoto M, Kohno M. Characterization of the bone morphogenetic protein-2 as a neurotrophic factor: induction of neuronal differentiation of PC12 cells in the absence of mitogen-activated protein kinase activation. J Biol Chem 1996;271:17360–5.
30. Nakamura Y, Ozaki T, Koseki H, Nakagawara A, Sakiyama S. Accumulation of p27 KIP1 is associated with BMP2-induced growth arrest and neuronal differentiation of human neuroblastoma-derived cell lines. Biochem Biophys Res Commun 2003;307:206–13.
31. Arregui CO, Mas CR, Argarana CE, Barra HS. Tubulin tyrosine ligase: protein and mRNA expression in developing rat skeletal muscle. Dev Growth Differ 1997;39:167–78.
32. Eiserich JP, Estevez AG, Bamberg TV, Ye YZ, Chumley PH, Beckman JS, Freeman BA. Microtubule dysfunction by posttranslational nitrotyrosination of alpha-tubulin: a nitric oxide-dependent mechanism of cellular injury. Proc Natl Acad Sci USA 1999;96:6365–70.
33. Kalisz HM, Erck C, Plessmann U, Wehland J. Incorporation of nitrotyrosine into alpha-tubulin by recombinant mammalian tubulin-tyrosine ligase. Biochim Biophys Acta 2000;1481:131–8.
34. Bisig CG, Purro SA, Contin MA, Barra HS, Arce CA. Incorporation of 3-nitrotyrosine into the C-terminus of alpha-tubulin is reversible and not detrimental to dividing cells. Eur J Biochem 2002;269:5037–45.
35. Ischiropoulos H. Biological tyrosine nitration: a pathophysiological function of nitric oxide and reactive oxygen species. Arch Biochem Biophys 1998;3561–611.
36. Hensley K, Maidt ML, Yu Z, Sang H, Markesbery WR, Floyd RA. Electrochemical analysis of protein nitrotyrosine and dityrosine in the Alzheimer brain indicates region-specific accumulation. J Neurosci 1998;18:8126–32.
37. Beal MF, Ferrante RJ, Browne SE, Matthews RT, Kowall NW, Brown RH Jr. Increased 3-nitrotyrosine in both sporadic and familial amyotrophic lateral sclerosis. Ann Neurol 1997;42:644–54.
38. Ishida Y, Ichimura T, Sumi H, Horigome T, Omata S. Methylmercury alters the tyrosination status of tubulin in the brains of acutely intoxicated rats. Toxicology 1997;122:171–81.
39. Nakagawara A, Arima-Nakagawara M, Scavarda NJ, Azar CG, Cantor AB, Brodeur GM. Association between high levels of expression of the TRK gene and favorable outcome in human neuroblastoma. N Engl J Med 1993;328:847–54.

Decreased expression of the candidate tumor suppressor gene *ING1* is associated with poor prognosis in advanced neuroblastomas

MASATO TAKAHASHI[1,2], TOSHINORI OZAKI[1], SATORU TODO[2] and AKIRA NAKAGAWARA[1]

[1]Division of Biochemistry, Chiba Cancer Center Research Institute, 666-2 Nitona, Chuoh-ku, Chiba 260-8717;
[2]First Department of Surgery, Hokkaido University School of Medicine, N15 W7, Kita-ku, Sapporo 060-8638, Japan

Received January 27, 2004; Accepted March 30, 2004

Abstract. *ING1* has been identified as a novel candidate tumor suppressor gene using a genetic suppressor element (GSE) strategy. Ectopic expression of *ING1* in mammalian cultured cells causes cell cycle arrest and apoptosis through a p53-dependent and/or p53-independent pathway. However, there has been no report on the prognostic significance of the *ING1* expression level in human cancers, though the expression of the wild-type *ING1* gene is significantly decreased in breast, lymphoid and gastric cancers as compared with their corresponding normal tissues. In order to explore the possible involvement of *ING1* in tumorigenesis of neuroblastoma, we examined the expression levels of *ING1* mRNA in 32 primary neuroblastomas by using a quantitative real-time PCR. *ING1* mRNA was expressed independently of the disease stages. However, low levels of *ING1* mRNA were significantly associated with a poor prognosis (log-rank test, p=0.017). Multivariate analysis showed that the expression level of *ING1* was closely related to survival (p=0.020), even after controlling with age (p=0.008) or stage (p=0.025), while it was only marginally significant after controlling with *TrkA* expression (p=0.063). Mutation analysis revealed that there was no mutation or deletion of the *ING1* gene except 1 silent mutation at codon 188 in primary neuroblastomas examined. Taken together, our results suggest for the first time that a decreased level of *ING1* expression is a novel indicator of poor prognosis in advanced stages of neuroblastoma, and that ING1 may play a crucial role in genesis and progression of neuroblastoma.

Introduction

Neuroblastoma, which is derived from the sympathoadrenal lineage of the neural crest, is one of the most common pediatric solid tumors (1). Neuroblastoma is an enigmatic tumor and shows distinct biology in 2 subsets. A subset of tumors in early stages has favorable prognosis and usually occurs in patients <1 year of age. They have no amplification of the *MYCN* oncogene and often differentiate and/or regress spontaneously. In contrast, the other is a subset of tumors in the advanced stages with poor prognosis, which usually possesses *MYCN* amplification and allelic loss in the distal region of the short arm of chromosome 1. However, there is an intermediate type of neuroblastoma which displays advanced phenotypes but has no *MYCN* amplification (2). From the clinical point of view, the latter type of neuroblastoma is the most problematic, and it is quite difficult to decide which therapeutic strategy should be chosen.

ING1 has been identified as a novel candidate tumor suppressor gene by using a novel strategy, which combines a subtractive hybridization and *in vivo* selection system (genetic suppressor elements method, GSE) (3,4). The *ING1* gene encodes a nuclear protein with a molecular mass of 33 kDa, which exhibits no significant homology with known proteins filed in the public databases. According to the recent reports, there exist at least 3 *ING1* variants arising from alternative splicing of mRNA (5,6). It has been mapped to human chromosome 13q33-q34, the region of which is known to be involved in the progression of various cancers (7-10). Expression of *ING1* is regulated in a cell cycle-dependent manner, reaching a maximal level during the S-phase (11-13). Ectopic expression of *ING1* in certain mammalian cultured cells results in a cell cycle arrest at the G0/G1 phase, suggesting that ING1 acts as a potent growth regulator (4). Furthermore, the physical and functional interaction of ING1 with tumor suppressor p53 has been reported and this could be one of the key mechanisms of the p53-mediated growth regulation (14). In addition, mutation of *ING1* which generates a truncated protein has been found in one of the neuroblastoma cell lines (4), suggesting that ING1 might be involved in genesis and/or progression of neuroblastoma.

To confirm this possibility, we performed mutation analysis of the *ING1* gene and also examined the expression levels of *ING1* mRNA in 32 primary neuroblastoma tissues. Although we did not detect any mutations or deletions, we found a significant decrease in the expression levels of *ING1* mRNA

Correspondence to: Dr Akira Nakagawara, Division of Biochemistry, Chiba Cancer Center Research Institute, 666-2 Nitona, Chuoh-ku, Chiba 260-8717, Japan
E-mail: akiranak@chiba-ccri.chuo.chiba.jp

Key words: ING1, neuroblastoma, p53, prognostic factor

in neuroblastoma tissues derived from patients who died of the disease. Thus, our present study suggests that the decreased level of *ING1* expression is a novel indicator of poor prognosis in advanced neuroblastoma.

Materials and methods

Patients and tumor tissues. Among 32 samples, 11 cases were identified by a mass screening program for neuroblastoma that began in 1985 in Japan. Eight tumors were obtained from patients treated at the Pediatric Oncology Group Institutions or other institutions in the United States. All tumors were diagnosed by histologic assessment. These consisted of 4 ganglioneuroblastomas and 28 neuroblastomas, all of which were considered neuroblastomas in these analyses. Staging was performed according to the staging system described by Evans *et al* (15), and identified 9 stage I, 4 stage II, 7 stage III, 5 stage IV and 7 stage IVs. All of the patients were treated according to previously described protocols (16-20). Despite differences between the protocols for the Japanese patients and those for the patients treated by the Pediatric Oncology Group, drugs and their doses were similar and the stage-specific survival rates obtained by these 2 groups did not differ significantly (data not shown). The median follow-up period after diagnosis was 26 months (range, 7-63). None of the patients underwent bone marrow transplantation.

Southern hybridization. The *MYCN* gene amplification was examined by Southern analysis. High molecular weight genomic DNA prepared from frozen neuroblastoma tissues was digested completely with *Eco*RI, separated by 1% agarose gel electrophoresis and transferred onto a nylon membrane filter. The filter was fixed by UV irradiation and hybridized at 42°C in a solution containing 6X SSC, 5x Denhardt's solution, 0.5% SDS and ^{32}P-labeled *MYCN* DNA. After hybridization, the filter was washed extensively at 50°C in 0.1X SSC containing 0.1% sarcosine and exposed to X-ray film with an intensifying screen at -70°C. The *MYCN* copy number was determined as described previously (21).

Northern blot analysis. Total RNA was extracted from 0.5-1.0 g of frozen neuroblastoma tissues using a standard guanidine thiocyanate extraction procedure (22). Total RNA (20 μg) was electrophoresed in 1% agarose gel under denaturing conditions and transferred by capillary onto nylon membrane filters. Hybridization was conducted at 42°C under the standard conditions in 6X SSC, 5X Denhardt's solution, 0.5% SDS and a radio-labeled cDNA probe for *TrkA* and *p53*. After hybridization, filters were washed at room temperature in 2X SSC/0.1% sarcosine followed by 2 washes at 50°C in 0.1X SSC containing 0.1% sarcosine and then exposed to X-ray film with an intensifying screen at -70°C. To normalize the expression level of genes of interest, filters were stripped of probes and rehybridized with a radio-labeled cDNA encoding *ß-actin*. The intensity of each specific band was measured by a densitometric scanning, and the expression level of each gene was expressed as arbitrary density units. The distinction between high and low level of *TRK-A* expression was based on the value of the histogram that gave the best natural separation (23).

Quantitative RT-PCR analysis. The expression level of *ING1* was measured by a real-time RT-PCR method (24). Total RNA (2 μg) was converted to first-strand cDNA using Superscript II reverse transcriptase (Life Technologies, Rockville, MD, USA). The PCR amplification was performed with the following primers: *ING1* sense (725F) (5'-AGATGATCGGCTGCGAC AA-3') and antisense (1038R) (5'-TCCCTATGAAAGGA ATGGTTCC-3'). The probe oligonucleotide (952T) (5'-TACATTGCCTTTGTTGAGGTGCAT-3') which hybridizes with the target sequences of the PCR products, was labeled with a reporter fluorescent dye (FAM, 6-carboxy-fluorescein) and a quencher fluorescent dye (TAMRA, 6-carboxytetramethyl-rhodamine) at its 5'- and 3'-end, respectively. PCR was carried out in a 25 μl reaction mixture containing 0.2 μM of each primer, 0.3 mM dATP, 0.3 mM dGTP, 0.3 mM dCTP, 0.6 mM dUTP instead of dTTP, 4 mM $Mn(OAc)_2$, 1X TaqMan EZ Buffer A, 0.25 units of AmpErase uracil N-glycosylase, 0.625 units of AmpliTaq Gold and 0.1 μM probe oligonucleotide. Reaction mixtures were pre-incubated at 50°C for 2 min, 95°C for 5 min and then subjected to 40 cycles of 95°C for 20 sec and 62°C for 1 min using ABI Prism 7700 Sequence Detector (PE Applied Biosystems). During the PCR amplification, the fluorescent-labeled probe was hydrolyzed by the activity of AmpliTaq Gold and the reporter dye was released from the probe oligonucleotide. The resulting increase in the reporter fluorescent emission was monitored in real-time. The expression level of *ING1* was normalized to that of *ß-actin* which was detected by the same real-time RT-PCR method.

RT-PCR SSCP analysis and DNA sequencing. For the detection of *ING1* mutation, we designed 4 primer sets which cover the entire coding region of human *ING1*. the reaction mixture contained 1 μl of the cDNA synthesized, 1 μM of each primer, 200 nM dNTPs, 1X reaction buffer, 0.15 units DNA polymerase (Expand High Fidelity PCR system) and [α-^{32}P]dCTP. PCR was performed as follows: pre-heating at 96°C for 3 min followed by 35 cycles of 96°C for 30 sec, 56°C for 30 sec and 72°C for 30 sec with final extension at 72°C for 5 min. PCR products were mixed with 1/10 volume of a loading buffer containing 95% formamide, 20 mM EDTA, 0.05% bromophenol blue and 0.05% xylene cyanol, denatured at 98°C for 5 min, and quenched on ice. Electrophoresis was carried out on 5% polyacrylamide gel with 5% glycerol at room temperature at 200 V for 15 h. After electrophoresis, the gel was dried and exposed to X-ray film with an intensifying screen at -70°C.

To determine nucleotide sequences of PCR products, they were purified by the GenElute Agarose Spin Column (Supelco, Bellefonte, PA, USA), subcloned into pGEM-T Easy Vector (Promega, Madison, WI, USA), and sequenced by the dideoxy chain termination method using the ABI Prism 377 DNA sequencer (Perkin-Elmer, Foster City, CA, USA).

Statistical analysis. A possible association between the *ING1* expression level and all prognostic factors was investigated using the Mann-Whitney U test. Pearson correlation with Bonferroni-adjusted significance levels were calculated between expression levels of all genes examined. Since the values of mRNA expression were skewed, a log or Box-cox

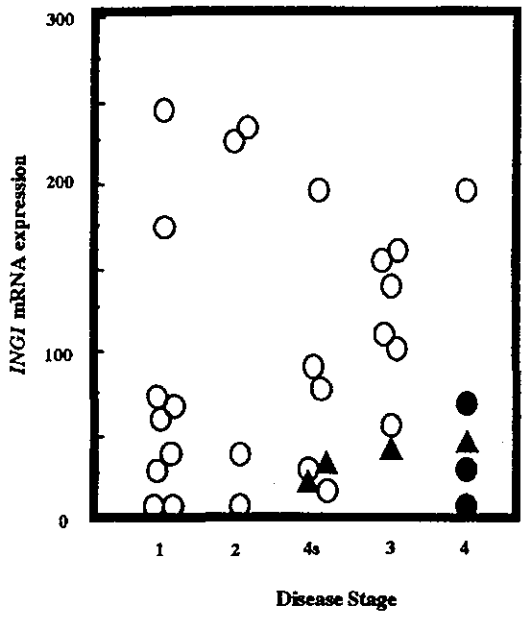

Figure 1. Expression of *ING1* mRNA in primary neuroblastomas. Total RNA was prepared from the indicated primary neuroblastoma tissues, and subjected to a quntitative real-time RT-PCR analysis as described under Materials and methods. The ratios of *ING1* mRNA levels to *β-actin* mRNA levels were quantified and are indicated as a fold change on the y axis. Nine in stage I, 4 in stage II, 7 in stage III, 5 in stage IV and 7 in stage IVs. (○), alive; (●), dead with single copy of *MYCN*; (▲), dead with *MYCN* amplification.

transformation was used to achieve the normality when calculating correlation coefficients. Comparisons between 2 clinical or biological variables were carried out using the χ^2 analysis. The Kaplan-Meier life table analysis was applied to compare individual variables and survival, and different survival curves were compared using the log-rank test. Cox regression models were used to explore the association between the expression of *ING1* and age, tumor stage, *MYCN*, *TRK-A* or survival. We considered $p>0.05$ to be significant. Statistical analyses were performed using the StatView version 4.5 (Abacus Concept Inc. Berkeley, CA, USA) and Stata version 6.0. (Stata Corporation, TX, USA).

Results

Mutation analysis of ING1 gene in human neuroblastoma. Recently, it has been reported that one of the human neuroblastoma cells, SK-N-SH, carries a mutation of the *ING1* gene, which generates a truncated form of *ING1* (4). To search for mutation of the *ING1* gene in 32 primary neuroblastoma tissues, we performed RT-PCR-single strand conformation polymorphism (SSCP) analysis, followed by subsequent DNA sequencing according to the procedure as described previously (25,26). Among 32 samples examined, the PCR product amplified from 1 case of neuroblastoma in stage I displayed an aberrantly migrating band, however, DNA sequencing analysis revealed that this aberrant band reflected a silent mutation at codon 188 [Ser188Ser (TCG-TCA)] (data not shown).

Down-regulation of ING1 mRNA is associated with unfavorable prognosis of neuroblastoma. We then examined

Table I. The results of log-rank tests for conventional prognostic factors and expression of *ING1* and *p53* in 32 primary neuroblastomas.

Variable	Number of subjects	Number of deaths (%)	Number of expected deaths	p-value
ING1 expression				.017
Low	16	6 (37.5)	2.96	
High	16	1 (6.3)	4.04	
p53 expression				.250
Not expressed	7	2 (28.6)	0.98	
Expressed	22	3 (13.6)	4.02	
Age				.001
<1 year	19	1 (5.3)	4.93	
>1 year	12	6 (50.0)	2.07	
Origin				.077
Adrenal gland	24	7 (100)	4.89	
Others	8	0 (0)	2.11	
Disease stage				.044
I+II+IVs	20	2 (10.0)	4.53	
III+IV	12	5 (41.7)	2.47	
MYCN copy number				<.0001
Amplified	4	4 (100)	0.39	
Single copy	28	3 (10.7)	6.61	
Trk-A expression				.0032
Low	6	3 (50.0)	0.78	
High	24	2 (8.3)	4.28	

ING1 expression levels in primary neuroblastomas because epigenetic regulation of the tumor suppressor genes are involved in the genesis and/or progression of many human cancers (27). Since the expression levels of *ING1* mRNA were below the detectable levels by Northern blot hybridization, we performed a quantitative real-time RT-PCR (24) to measure its expression levels in 32 neuroblastoma tissues. The threshold cycle number value (C_T), indicating the relative levels of *ING1* mRNA (after normalization to that of *β-actin* mRNA) was in the range of 0-250 (median value, 64). As shown in Fig. 1, there were no statistically significant differences in expression levels of *ING1* mRNA among the disease stages (mean ± SEM; stage I, 79±27, n=9; stage II, 126±59, n=4; stage IVs, 67±24, n=7; stage III, 110±17, n=7; stage IV, 70±33, n=5; $p>0.05$). Note that *ING1* expression levels were significantly decreased in the tumors obtained from the patients who died of the disease (mean ± SEM; 36±8, n=7) as compared with those patients who were alive (101±15, n=25) (Mann-Whitney U test, $p=0.043$). Then, the patients were divided into 2 groups according to the median value of *ING1* mRNA expression in the tumor. The log-rank test showed that the prognosis of the patients with decreased expression of *ING1* was significantly poor ($p=0.017$) (Table I and Fig. 2).

The expression of p53 was not correlated with the prognosis of neuroblastoma. Since ING1 has been shown to modulate the function of p53 through the physical interaction with p53

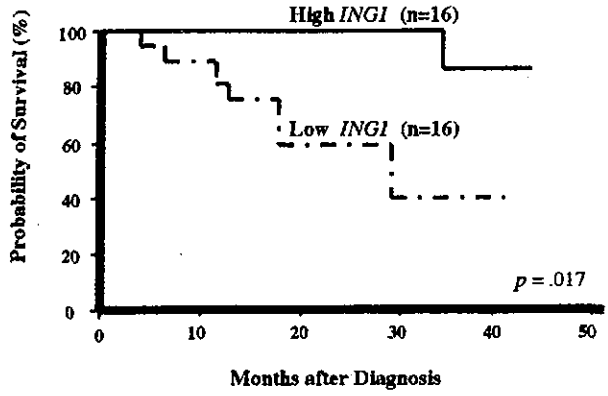

Figure 2. *ING1* mRNA expression and survival curves calculated by the Kaplan-Meier method. Kaplan-Meier life table analysis was used to compare the individual variables and survival, and different survival curves were compared using the *log-rank* test. Statistical analyses were performed using the StatView viersion 4.5 and Stata version 6.0. (—), A group of patients with high levels of *ING1* expression; (-•-•-), a group of patients with low levels of *ING1* expression.

Table II. Cox regression models using dichotomous factors of age, disease stage, *MYCN* amplification and expression of *Trk-A* and *ING1*.

Factor	n	p-value	HR (95% CI)
Age (≥1 vs. <1 year)	31	.013	14.6 (1.75-121)
Stage (III+IV vs. I+II+IVs)	32	.069	4.6 (0.89-23.6)
MYCN ampl. (>1 vs. 1 copy)	32	<.0005	55.8 (6.01-518)
Trk-A exp. (low vs. high)	30	.016	9.4 (1.53-57.8)
ING1 exp. (low vs. high)	32	.046	9.0 (1.04-77.2)
ING1 exp. (low vs. high)	31	.022	27.1 (1.61-455)
Age (≥1 vs. <1 year)		.008	24.3 (2.32-255)
ING1 exp. (low vs. high)	32	.023	15.7 (1.47-167)
Stage (III+IV vs. I+II+IVs)		.025	7.7 (1.30-45.2)
ING1 exp. (low vs. high)	30	.063	12.9 (0.87-190)
Trk-A exp. (low vs. high)		.017	17.3 (1.68-179)

All variables with 2 categories; HR, hazard ratio shows the relative risk of death of first category relative to the second; CI, confidence interval.

(14), we also examined the expression levels of *p53* in the same neuroblastoma tissues by Northern blot hybridization. The expression of *ß-actin* mRNA served as an internal control, and the patients were divided into 2 groups with detectable (high) and undetectable (low) expression of *p53*. As shown in Table I, *p53* expression was not significantly associated with the prognosis of neuroblastoma (p=0.25). These results suggest that the decreased expression of *ING1* but not of *p53* is correlated with the unfavorable prognosis of neuroblastoma.

ING1 expression is an independent prognostic indicator for neuroblastoma. We then performed a multivariate analysis of the prognostic factors for neuroblastoma including *ING1* expression. As shown in Table II, the predictive importance of *ING1* expression for survival was demonstrated after controlling patient's age (p=0.022) and disease stage (p=0.023), whereas *ING1* expression was marginally significant (p=0.063) after controlling *TrkA* expression. This implied that *ING1* expression may be a prognostic indicator which is independent on age and stage, but that it may be weakly associated with *TrkA* expression in predicting the prognosis of neuroblastoma.

Discussion

In the present study, we have searched for mutations of the *ING1* gene, and examined the expression levels of *ING1* mRNA in 32 primary neuroblastoma tissues. Although we did not detect any mutations with amino acid substitutions, we found that the expression levels of *ING1* mRNA were significantly reduced in unfavorable neuroblastoma, and this marked down-regulation was associated with the poor prognosis of neuroblastoma. Our present results represent an initial step toward understanding the biological significance of *ING1* in neuroblastoma.

Recently, it has been shown that ING1 has an ability to promote cell cycle arrest and apoptosis in certain mammalian cultured cells (14,28). Garkavtsev *et al* found a truncated form of *ING1* protein in neuroblastoma cell lines, which might be generated by a structural rearrangement or a deletion that occurred within the *ING1* gene (4). It remains unknown whether the truncated ING1 protein retains the ability to inhibit cell cycle progression, and whether there exists a loss of function mutations of *ING1* in primary neuroblastoma, it is likely that ING1 might act as a candidate tumor suppressor for neuroblastoma. Consistent with the recent reports showing that *ING1* is rarely mutated in human malignancies (5,29-31), our mutation analysis indicated that *ING1* is infrequently mutated in primary neuroblastomas and thus it might not function as a tumor suppressor in the classic manner (32). Note that our quantitative real-time RT-PCR analysis revealed that the expression levels of *ING1* mRNA were reduced in unfavorable neuroblastomas, and that this down-regulation was significantly correlated with the poor prognosis of neuroblastoma. Although the number of tumor samples used in this study was relatively small, the statistical significance of the traditional prognostic factors including patient's age (p=0.001), disease stage (p= 0.044), *MYCN* amplification (p<0.0001) and *TrkA* expression (p=0.0032) were in good agreement with those reproducibly documented (15,33,34). Thus, our present results suggest that *ING1* expression is a novel prognostic indicator for neuroblastomas especially in advanced stages. In order to design a new therapeutic strategy against aggressive neuroblastoma, it will be necessary to clarify the molecular mechanisms of this transcriptional down-regulation of the *ING1* gene in unfavorable neuroblastoma.

There is considerable evidence that the p53 pathway is not exclusively responsible for the genesis and/or progression of neuroblastoma. For example, *p53* is infrequently mutated in primary neuroblastomas, and wild-type p53 is localized largely in cytoplasm of primary tumors as well as neuroblastoma-derived cell lines (35-39). In addition, our present study indicated that the expression levels of *p53* mRNA is not associated with the prognosis of neuroblastoma. On the other hand, it has been shown that p53 plays an important

role in inducing neuronal cell death of sympathetic neurons, from which neuroblastoma originates (40). Recently, Nakagawa *et al* reported that during cisplatin-mediated cell death in neuroblastoma-derived SH-SY5Y cells, endogenous p53 accumulated at a protein level, suggesting that the p53 pathway is closely involved in DNA damage-induced neuroblastoma cell death (41). Previous studies have demonstrated that ING1 physically interacts with p53, and thereby acts as a cofactor of p53 to enhance its ability to transactivate downstream target genes as well as to inhibit cell cycle progression (14,42). It is likely that the reduced expression of *ING1* could down-regulate the pro-apoptotic function of p53 and thereby promote neuroblastoma cell growth. To confirm this possibility, further studies are necessary.

Acknowledgements

We are grateful to S. Sakiyama and S. Ichimiya for valuable discussions, and A. Morohashi for preparing RNA. We thank Y. Nakamura and M. Nagano for assistance in quantitative RT-PCR analysis. This work was supported in part by a Grant-in-Aid from the Ministry of Health and Welfare for a New 10-Year Strategy for Cancer Control, a Grant-in-Aid from the Ministry of Health and Welfare for the Study Group for Treatment of Advanced Neuroblastoma, Uehara Foundation, and a Grant-in-Aid for Scientific Research from the Ministry of Education, Science, Sports and Culture, Japan. Masato Takahashi is an awardee of the Research Resident Fellowship from the Foundation for Promotion of Cancer Research in Japan.

References

1. Bolande R: The neurocristopathies: a unifying concept of disease arising in neural crest maldevelopment. Human Pathol 5: 409-424, 1974.
2. Brodeur GM and Nakagawara A: Molecular basis of clinical heterogeneity in neuroblastoma. Am J Pediatr Hematol Oncol 14: 111-116, 1992.
3. Roninson IB, Gudkov AV, Holzmayer TA, Kirschling DJ, Kazarov AR, Zelnick CR, Mazo IA, Axenovich S and Thimmapaya R: Genetic suppressor elements: new tools for molecular oncology - Thirteenth Cornelius P. Rhoads Memorial Award Lecture. Cancer Res 55: 4023-4028, 1995.
4. Garkavtsev I, Kazarov A, Gudkov A and Riabowol K: Suppression of the novel growth inhibitor p33*ING1* promotes neoplastic transformation. Nat Genet 14: 415-420, 1996.
5. Gunduz M, Ouchida M, Fukushima K, Hanafusa H, Etani T, Nishioka S, Nishizaki K and Shimizu K: Genomic structure of the human *ING1* gene and tumor-specific mutations detected in head and neck squamous cell carcinomas. Cancer Res 60: 3143-3146, 2000.
6. Saito A, Furukawa T, Fukushige S, Koyama S, Hoshi M, Hayashi Y and Horii A: p24/*ING1*-ALT1 and p47/*ING1*-ALT2, distinct alternative transcripts of p33/*ING1*. J Hum Genet 45: 177-181, 2000.
7. Motomura K, Nishisho I, Takai S, Tateishi H, Okazaki M, Yamamoto M, Miki T, Honjo T and Mori T: Loss of alleles at loci on chromosome 13 in human primary gastric cancers. Genomics 2: 180-184, 1988.
8. Ried T, Petersen I, Holtgreve-Grez H, Speicher MR, Schrock E, du Manoir S and Cremer T: Mapping of multiple DNA gains and losses in primary small cell lung carcinomas by comparative genomic hybridization. Cancer Res 54: 1801-1806, 1994.
9. Maestro R, Piccinin S, Doglioni C, Gasparotto D, Vukosavljevic T, Sulfaro S, Barzan L and Boiocchi M: Chromosome 13q deletion mapping in head and neck squamous cell carcinomas: identification of two distinct regions of preferential loss. Cancer Res 56: 1146-1150, 1996.
10. Hyytinen ER, Frierson HF Jr, Boyd JC, Chung LW and Dong JT: Three distinct regions of allelic loss at 13q14, 13q21-22, and 13q33 in prostate cancer. Genes Chromosomes Cancer 25: 108-114, 1999.
11. Garkavtsev I, Demetrick D and Riabowol K: Cellular localization and chromosome mapping of a novel candidate tumor suppressor gene (*ING1*). Cytogenet Cell Genet 76: 176-178, 1997.
12. Zeremski M, Horrigan SK, Grigorian IA, Westbrook CA and Gudkov AV: Localization of the candidate tumor suppressor gene *ING1* to human chromosome 13q34. Somat Cell Mol Genet 23: 233-236, 1997.
13. Garkavtsev I and Riabowol K: Extension of the replicative life span of human diploid fibroblasts by inhibition of the p33*ING1* candidate tumor suppressor. Mol Cell Biol 17: 2014-2019, 1997.
14. Garkavtsev I, Grigorian IA, Ossovskaya VS, Chernov MV, Chumakov PM and Gudkov AV: The candidate tumour suppressor p33*ING1* cooperates with p53 in cell growth control. Nature 391: 295-298, 1998.
15. Evans AE, D'Angio GJ and Randolph J: A proposed staging for children with neuroblastoma. Children's cancer study group A. Cancer 27: 374-378, 1971.
16. Ikeda K, Nakagawara A, Yano H, Akiyama H, Tasaka H, Ueda K, Hara T, Ishii E, Ohgami H, Sera Y, *et al*: Improved survival rates in children over 1 year of age with stage III or IV neuroblastoma following an intensive chemotherapeutic regimen. J Pediatr Surg 24: 189-193, 1989.
17. Nitschke R, Smith EI, Altshuler G, Altmiller D, Shuster J, Green A, Castleberry R, Hayes FA, Golembe B and Ducos R: Postoperative treatment of nonmetastatic visible residual neuroblastoma: a Pediatric Oncology Group study. J Clin Oncol 9: 1181-1188, 1991.
18. Castleberry RP, Kun LE, Shuster JJ, Altshuler G, Smith IE, Nitschke R, Wharam M, McWilliams N, Joshi V and Hayes FA: Radiotherapy improves the outlook for patients older than 1 year with Pediatric Oncology Group stage C neuroblastoma. J Clin Oncol 9: 789-795, 1991.
19. Look AT, Hayes FA, Shuster JJ, Douglass EC, Castleberry RP, Bowman LC, Smith EI and Brodeur GM: Clinical relevance of tumor cell ploidy and N-myc gene amplification in childhood neuroblastoma: a Pediatric Oncology Group study. J Clin Oncol 9: 581-591, 1991..
20. Hirai M, Yoshida S, Kashiwagi H, Kawamura T, Ishikawa T, Kaneko M, Ohkawa H, Nakagawara A, Miwa M and Uchida K: 1q23 gain is associated with progressive neuroblastoma resistant to aggressive treatment. Genes Chromosomes Cancer 25: 261-269, 1999.
21. Brodeur GM, Seeger RC, Schwab M, Varmus HE and Bishop JM: Amplification of N-myc in untreated human neuroblastomas correlates with advanced disease stage. Science 224: 1121-1124, 1984.
22. Chomczynski P and Sacchi N: Single-step method of RNA isolation by acid guanidinium thiocyanate-phenol-chloroform extraction. Anal Biochem 162: 156-159, 1987.
23. Nakagawara A, Arima M, Azar CG, Scavarda NJ and Brodeur GM: Inverse relationship between trk expression and N-myc amplification in human neuroblastomas. Cancer Res 52: 1364-1368, 1992.
24. Heid CA, Stevens J, Livak KJ and Williams PM: Real-time quantitative PCR. Genome Res 6: 986-994, 1996.
25. Ichimiya S, Nimura Y, Kageyama H, Takada N, Sunahara M, Shishikura T, Nakamura Y, Sakiyama S, Seki N, Ohira M, Kaneko Y, McKeon F, Caput D and Nakagawara A: p73 at chromosome 1p36.3 is lost in advanced stage neuroblastoma but its mutation is infrequent. Oncogene 18: 1061-1066, 1999.
26. Sunahara M, Shishikura T, Takahashi M, Todo S, Yamamoto N, Kimura H, Kato S, Ishioka C, Ikawa S, Ikawa Y and Nakagawara A: Mutational analysis of p51A/TAp63gamma, a p53 homolog, in non-small cell lung cancer and breast cancer. Oncogene 18: 3761-3765, 1999.
27. Jirtle RL: Genomic imprinting and cancer. Exp Cell Res 248: 18-24, 1999.
28. Helbing CC, Veillette C, Riabowol K, Johnston RN and Garkavtsev I: A novel candidate tumor suppressor, *ING1*, is involved in the regulation of apoptosis. Cancer Res 57: 1255-1258, 1997.
29. Toyama T, Iwase H, Watson P, Muzik H, Saettler E, Magliocco A, DiFrancesco L, Forsyth P, Garkavtsev I, Kobayashi S and Riabowol K: Suppression of *ING1* expression in sporadic breast cancer. Oncogene 18: 5187-5193, 1999.

30. Campos EI, Cheung KJ Jr, Murray A, Li S and Li G: The novel *tumour suppressor gene ING1 is overexpressed* in human melanoma cell lines. Br J Dermatol 146: 574-580, 2002.
31. Chen B, Campos EI, Crawford R, Martinka M and Li G: Analyses of the tumour suppressor *ING1* expression and gene mutation in human basal cell carcinoma. Int J Oncol 22: 927-931, 2003.
32. Knudson AG Jr: Mutation and cancer: statistical study of retinoblastoma. Proc Natl Acad Sci USA 68: 820-823, 1971.
33. Coldman AJ, Fryer CJ, Elwood JM and Sonley MJ: Neuroblastoma: influence of age at diagnosis, stage, tumor site, and sex on prognosis. Cancer 46: 1896-1901, 1980.
34. Nakagawara A, Arima-Nakagawara M, Scavarda NJ, Azar CG, Cantor AB and Brodeur GM: Association between high levels of expression of the TRK gene and favorable outcome in human neuroblastoma. N Engl J Med 328: 847-854, 1993.
35. Vogan K, Bernstein M, Leclerc JM, Brisson L, Brossard J, Brodeur GM, Pelletier J and Gros P: Absence of p53 gene mutations in primary neuroblastomas. *Cancer Res 53: 5269-5273*, 1993.
36. Castresana JS, Bello MJ, Rey JA, Nebreda P, Queizan A, Garcia-Miguel P and Pestana A: No TP53 mutations in neuroblastomas detected by PCR-SSCP analysis. Genes Chromosomes Cancer 10: 136-138, 1994.
37. Hosoi G, Hara J, Okamura T, Osugi Y, Ishihara S, Fukuzawa M, Okada A, Okada S and Tawa A: Low frequency of the p53 gene mutations in neuroblastoma. Cancer 73: 3087-3093, 1994.
38. Keshelava N, Zuo JJ, Chen P, Waidyaratne SN, Luna MC, Gomer CJ, Triche TJ and Reynolds CP: Loss of p53 function confers high-level multidrug resistance in neuroblastoma cell lines. Cancer Res 61: 6185-6193, 2001.
39. Moll UM, LaQuaglia M, Benard J and Riou G: Wild-type p53 protein undergoes cytoplasmic sequestration in undifferentiated neuroblastomas but not in differentiated tumors. Proc Natl Acad *Sci USA 92: 4407-4411*, 1995.
40. Aloyz RS, Bamji SX, Pozniak CD, Toma JG, Atwal J, Kaplan DR and Miller FD: p53 is essential for developmental neuron death as regulated by the TrkA and p75 neurotrophin receptors. J Cell Biol 143: 1691-1703, 1998.
41. Nakagawa T, Takahashi M, Ozaki T, Watanabe Ki K, Todo S, Mizuguchi H, Hayakawa T and Nakagawara A: Autoinhibitory regulation of p73 by Delta Np73 to modulate cell survival and death through a p73-specific target element within the Delta Np73 promoter. Mol Cell Biol 22: 2575-2585, 2002.
42. Takahashi M, Seki N, Ozaki T, Kato M, Kuno T, Nakagawa T, Watanabe K, Miyazaki K, Ohira M, Hayashi S, Hosoda M, Tokita H, Mizuguchi H, Hayakawa T, Todo S and Nakagawara A: Identification of the p33(*ING1*)-regulated genes that include cyclin B1 and proto-oncogene DEK by using cDNA microarray in a mouse mammary epithelial cell line NMuMG. Cancer Res 62: 2203-2209, 2002.

Oncogene (2004) 23, 5901–5911

www.nature.com/onc

Expression profiling and differential screening between hepatoblastomas and the corresponding normal livers: identification of high expression of the *PLK1* oncogene as a poor-prognostic indicator of hepatoblastomas

Shin-ichi Yamada[1], Miki Ohira[1], Hiroshi Horie[2], Kiyohiro Ando[1], Hajime Takayasu[1], Yutaka Suzuki[3], Sumio Sugano[3], Takahiro Hirata[4], Takeshi Goto[4], Tadashi Matsunaga[2], Eiso Hiyama[2], Yutaka Hayashi[2], Hisami Ando[2], Sachiyo Suita[2], Michio Kaneko[2], Fumiaki Sasaki[2], Kohei Hashizume[2], Naomi Ohnuma[2] and Akira Nakagawara*[,1,2]

[1]*Division of Biochemistry, Chiba Cancer Center Research Institute, Chiba 260-8717, Japan;* [2]*Japanese Study Group for Pediatric Liver Tumor, Japan;* [3]*Human Genome Center, Institute of Medical Science, University of Tokyo, Tokyo 108-8639, Japan;* [4]*Hisamitsu Pharmaceutical Co. Inc., Tokyo 100-6221, Japan*

Hepatoblastoma is one of the most common malignant liver tumors in young children. Recent evidences have suggested that the abnormalities in Wnt signaling pathway, as seen in frequent mutation of the *β-catenin* gene, may play a role in the genesis of hepatoblastoma. However, the precise mechanism to cause the tumor has been elusive. To identify novel hepatoblastoma-related genes for unveiling the molecular mechanism of the tumorigenesis, a large-scale cloning of cDNAs and differential screening of their expression between hepatoblastomas and the corresponding normal livers were performed. We constructed four full-length-enriched cDNA libraries using an oligo-capping method from the primary tissues which included two hepatoblastomas with high levels of alpha-fetoprotein (AFP), a hepatoblastoma without production of AFP, and a normal liver tissue corresponded to the tumor. Among the 10 431 cDNAs randomly picked up and successfully sequenced, 847 (8.1%) were the genes with unknown function. Of interest, the expression profile among the two subsets of hepatoblastoma and a normal liver was extremely different. A semiquantitative RT–PCR analysis showed that 86 out of 1188 genes tested were differentially expressed between hepatoblastomas and the corresponding normal livers, but that only 11 of those were expressed at high levels in the tumors. Notably, *PLK1* oncogene was expressed at very high levels in hepatoblastomas as compared to the normal infant's livers. Quantitative real-time RT–PCR analysis for the *PLK1* mRNA levels in 74 primary hepatoblastomas and 29 corresponding nontumorous livers indicated that the patients with hepatoblastoma with high expression of *PLK1* represented significantly poorer outcome than those with its low expression (5-year survival rate: 55.9 vs 87.0%, respectively, $p = 0.042$), suggesting that the level of *PLK1* expression is a novel marker to predict the prognosis of hepatoblastoma. Thus, the differentially expressed genes we have identified may become a useful tool to develop new diagnostic as well as therapeutic strategies of hepatoblastoma.
Oncogene (2004) **23**, 5901–5911. doi:10.1038/sj.onc.1207782
Published online 28 June 2004

Keywords: hepatoblastoma; expression profile; oligo-capping cDNA library; PLK1; prognostic factor

Introduction

Hepatoblastoma (HBL) is the most common hepatic cancer in children (Exelby *et al.*, 1975; Weinberg and Finegold, 1983). However, the etiology of HBL has been unclear in contrast to the adult hepatocellular carcinoma (HCC), in which preceding infection of hepatitis virus is often found (Buendia, 1992; Idilman *et al.*, 1998). Although most HBLs are sporadic, it is sometimes associated with certain hereditary diseases such as Beckwith–Wiedemann syndrome (Albrecht *et al.*, 1994) and familial adenomatous polyposis (Li *et al.*, 1987; Giardiello *et al.*, 1996; Kinzler and Vogelstein, 1996). In the former, loss of heterozygosity of chromosome 11p15.5 is frequently observed, and the abnormal regulation of the *insulin-like growth factor 2* (*IGF2*) and the *H19* genes at this locus may contribute to the disease (Albrecht *et al.*, 1994; Montagna *et al.*, 1994; Li *et al.*, 1995; Rainier *et al.*, 1995; Yun *et al.*, 1998; Fukuzawa *et al.*, 1999). In the latter, the *APC* gene, which is one of the key molecules in Wnt signaling, was found to be constitutively mutated (Kinzler and Vogelstein, 1996).

Increasing evidence suggests that Wnt signaling pathway also plays an important role in the genesis of sporadic hepatoblastomas. A high frequency (more than 60% in some reports) of somatic mutations in the *β-catenin* gene has recently been reported in sporadic tumors (Koch *et al.*, 1999; Wei *et al.*, 2000; Takayasu

*Correspondence: A Nakagawara, Division of Biochemistry, Chiba Cancer Center Research Institute, 666-2 Nitona, Chiba 260-8717, Japan; E-mail: akiranak@chiba-ccri.chuo.chiba.jp
Received 9 December 2003; revised 26 March 2004; accepted 1 April 2004; published online 28 June 2004

et al., 2001; Buendia, 2002). Mutant β-catenin proteins accumulate in the nucleus, resulting in stimulating transcription of the target genes such as *c-myc* and *cyclin D1* (Morin *et al.*, 1997; Polakis, 1999). Mutation in the *Axin* gene, whose product is an antagonist of nuclear accumulation of β-catenin, has also been found in HBL and may contribute to the pathogenesis of the tumors without *β-catenin* mutation (Taniguchi *et al.*, 2002; Miao *et al.*, 2003). However, the molecular mechanism underlying the pathogenesis of HBL is still largely unknown.

Recent progress in therapeutic strategies including intensive chemotherapy and liver transplantation improved the outcome of the patients with HBL. However, the prognosis of a significant fraction of the tumors still remains poor. The clinical markers currently used for HBL include staging, which is a major instrument for assessing prognosis (Hata, 1990), serum alpha-fetoprotein (AFP) (Mann *et al.*, 1978), mitotic activity (Haas *et al.*, 1989), DNA ploidy (Hata *et al.*, 1991), nuclear localization of β-catenin (Park *et al.*, 2001), p53 mutation (Oda *et al.*, 1995), and chromosomal alteration (Weber *et al.*, 2000). Serum AFP level is used as a diagnostic marker to monitor the tumor progression, responsiveness to the therapy, and recurrence after the treatment. Extremely high levels of serum AFP are reported to be associated with aggressiveness of the tumors with unfavorable outcome (van Tornout *et al.*, 1997), except some reports showing that there is no significant relationship between initial serum AFP levels and prognosis of the patients with HBL (Ortega *et al.*, 1991; von Schweinitz *et al.*, 1994). Moreover, the tumor with low levels of serum AFP often grows rapidly and is often reluctant to chemotherapy (von Schweinitz *et al.*, 1995). The other genetic markers including DNA ploidy, chromosomal aberration, and *p53* mutation are not so powerful clinical indicators. Even the nuclear localization of β-catenin and/or mutation of the *β-catenin* gene appear to lose their impact as a prognostic factor when combined with the grade of histological differentiation because of its close correlation with the latter (Takayasu *et al.*, 2001). Therefore, we may need to find novel markers to predict the patient's outcome in a comprehensive way.

To understand the molecular mechanism of the genesis and progression of HBL, as well as to develop a novel diagnostic and therapeutic system for the tumor, we have randomly cloned 10431 cDNAs expressed in primary HBL tissues and a normal infant's liver by using full-length-enriched oligo-capping cDNA libraries. In the present study, we have identified 86 genes differentially expressed between HBLs and their corresponding normal livers. One of such genes, *PLK1*, showed a significantly high expression in the formers as compared with the latters, and its high expression was significantly associated with poor prognosis of HBLs.

Results

Expression profiles of primary HBLs and a normal liver

To obtain the genes expressed in primary HBLs and normal infant's liver, we constructed oligo-capping cDNA libraries from two primary HBLs with increased AFP secretion (HMFT, HYST), a primary HBL without AFP secretion (HKMT), and a corresponding normal liver (HMFN). After cloning 3000 cDNAs from each of the four cDNA libraries, 2289, 2837, 2537, and 2768 clones from the libraries of HMFT, HYST, HKMT, and HMFN, respectively, were successfully end-sequenced. Homology search against the public databases of those 10431 clones by BLAST program revealed that 847 clones (8.1%) in total contained novel sequences which had not been annotated (Table 1).

To elucidate the gene expression pattern in each cDNA library, we compared expression profile of the known genes that appeared in three different kinds of libraries, a HBL with positive AFP (HMFT), a HBL with negative AFP (HKMT), and an infant's liver (HMFN) (Table 2). BodyMap (Okubo *et al.*, 1992) and a serial analysis of gene expression (SAGE) (Velculescu *et al.*, 2000) are very good methods to quickly provide quantification of the levels of all mRNAs in certain tissues and cell types by high throughput end-sequencing of cDNA clones. In this study, we applied the former method by counting cDNA clones to show each expression profile of HBL tumors or a non-tumorous tissue. Although each library consists of 3000 clones, which may be a rather small number, the frequency of each cDNA appearance provides a hint to understand each tissue's genetic background.

Overall, the most frequently appeared gene was *albumin* as expected, which was extremely low in the tumor with negative AFP. Genes involved in cellular structure and/or maintenance, glucose and lipid metabolisms, and a part of protein synthesis and its transport were frequently found in the normal liver library. On the

Table 1 Summary of the number of genes cloned from the cDNA libraries of hepatoblastomas and a normal infant liver of hepatoblastomas

Oligo-capping cDNA library	*No. of the clones*	*No. of the genes successfully end-sequenced*	*No. of the genes with unknown function*
Hepatoblastomas with positive AFP	6000	5126	323 (6.3%)
Hepatoblastoma with negative AFP	3000	2537	262 (10.3%)
Infant's liver	3000	2768	262 (9.5%)
Total	12000	10431	847 (8.1%)

Table 2 Comparison of the known genes frequently appeared in hepatoblastomas with or without secretion of AFP and a non-tumorous infant's liver

Gene symbol	*Acc. no.*	*Gene name*	*No. of appearance of the genes*		
			HBL with positive AFP	*Normal infant's liver*	*HBL with negative AFP*
Total number of genes			2289	2768	2537
Protein synthesis, metabolism, transport					
ALB	NM_000477	Albumin	558	482	8
AFP	NM_001134	Alpha-feto protein	67	0	0
AGT	NM_000029	Angiotensinogen	43	16	0
EEF1A1	X03558	Eukaryotic translation elongation factor 1 alpha 1	35	20	87
RPL27A	NM_000990	60S ribosomal protein L27a	31	4	52
FTL	M11147	Ferritin	24	11	3
FGA	NM_021871	Fibrinogen, A alpha polypeptide	20	38	2
HP	K01763	Haptoglobin	19	6	1
ORM1	X02544	Orosomucoid-1	12	8	0
RPS27	NM_001030	Ribosomal protein S27	11	4	31
F2	J00307	Coagulation factor 2	11	26	0
TF	NM_001063	Transferrin	8	6	0
PAH	U49897	Phenylalanine hydroxylase	6	6	0
PLG	NM_000301	Plasminogen	5	8	0
SERPINA1	X01683	Serine proteinase inhibitor, clade A, member 1	5	6	0
GC	NM_000583	Group-specific component	4	21	1
RPS29	NM_001032	Ribosomal protein S29	3	1	0
CTSB	NM_147783	Cathepsin B	2	5	3
SERPING1	BC011171	Serine proteinase inhibitor, clade G, menber 1	2	33	0
CRP	X56692	C-reactive protein	1	8	0
ITIH2	NM_002216	Inter-alpha (globulin) inhibitor, H2 polypeptide	0	25	0
Growth factor					
MST1	M74178	Macrophage stimulating 1	8	16	0
Cell signaling					
WIF1	NM_007191	Wnt inhibitory factor 1	0	0	11
DKK1	NM_012242	Dickkopf	0	0	7
Cell structure, adhesion					
VTN	NM_000638	Vitronectin	7	30	0
ACTB	BC013380	Actin	6	17	6
LRG	AF403428	Leucine-rich alpha-2-glycoprotein	6	11	0
VIM	NM_003380	Vimentin	0	3	38
Cell cycle					
RBM4	NM_002896	RNA binding motif protein	2	0	21
RAP1B	NM_015646	RAP1B	0	0	11
Organism defense					
BF	L15702	B-factor, properdin	5	13	0
GPX1	NM_000581	Glutathione peroxidase	4	0	0
C1R	NM_001733	Complement component 1	1	21	1
Glycometabolism					
LDHA	NM_005566	Lactate dehydrogenase	19	28	7
ADH1B	AF153821	Alcohol dehydrogenase	15	29	1
CES1	L07764	Carboxylesterase	9	22	2
ALDH1A1	NM_000689	Aldehyde dehydrogenase	2	13	2
Lipid metabolism					
EPHX1	NM_000120	Epoxide hydrolase 1	7	12	0
APOA2	NM_001643	Apolipoprotein A-II	6	2	0
ADFP	BC005127	Adipose differentiation-related protein	5	14	1
Heat shock protein, metabolic enzyme					
UGT2B4	Y00317	UDP-glucuronosyltransferase	11	32	2
HSPA8	NM_006597	Heat shock 70 kDa protein	1	6	1
Unknown, others					
ATP5A1	NM_004046	ATP synthase	18	11	23
SEPP1	NM_005410	Selenoprotein P	7	10	2

Table 2 (*continued*)

Gene symbol	*Acc. no.*	*Gene name*	*No. of appearance of the genes*		
			HBL with positive AFP	*Normal infant's liver*	*HBL with negative AFP*
CYP3A4	M18907	P450	6	81	3
AHSG	M16961	Alpha-2-HS-glycoprotein	6	5	2
TPT1	X16064	Translationally controlled tumor protein	6	0	3
CYP2C9	M61855	P4502C9	1	10	1

other hand, genes involved in protein synthesis such as elongation factors and ribosomal proteins were observed more frequently in HBLs than in normal liver. The expression profile in the library of the tumor without AFP secretion was very different from that with positive AFP (HMFT *vs* HKMT). As expected, *AFP* gene did not appear in the HKMT library. Intriguingly, *Wnt Inhibitory factor-1* and *dickkopf*, both of which are inhibitors of Wnt signaling (Hsieh *et al*., 1999; Wang *et al*., 2000), frequently appeared in the HKMT library. In addition, *vimentin*, *RNA-binding motif protein*, and *RAP1B* also frequently appeared in the HKMT library, but hardly in the HMFT library with AFP secretion. Thus, HBL with positive AFP and that with negative AFP seem to have a distinct gene expression profile, resulting in different biological characteristics.

Identification of the differentially expressed genes between HBLs and normal livers

To identify differentially expressed genes between HBLs and their corresponding normal livers, 1188 independent genes which included all of the 847 genes with unknown function and 341 known genes that were related to cellular functions including cell growth and differentiation among the 10431 cDNAs were selected and subjected to semiquantitative RT–PCR analysis (Figure 1a). The complementary DNAs reverse-transcribed from total RNA obtained from eight tumors and their corresponding normal livers were used as PCR templates after normalization with *GAPDH* expression. As a result, we found that 75 genes were expressed at higher levels in normal livers than in HBLs, whereas only 11 genes were expressed at higher levels in the tumors than in normal livers. Figure 1a shows the representatives of the results of differential screening using semi-quantitative RT–PCR and Table 3 lists 46 differentially expressed genes with known functions. We classified those differentially expressed genes into 12 categories according to their known functions. The genes preferentially expressed in normal liver showed the profiles which reflected normal liver function. Consistent with the previous reports about HBL and hepatocellular carcinoma (von Horn *et al*., 2001; Xu *et al*., 2001; Kinoshita and Miyata, 2002), *Insulin-like growth factor binding protein-3* (*IGFBP-3*), *aldolase B*, *ceruloplasmin*, and *c-reactive protein* were downregulated in HBLs as compared with the normal livers. The expression of *IGF2*, whose product has mitogenic

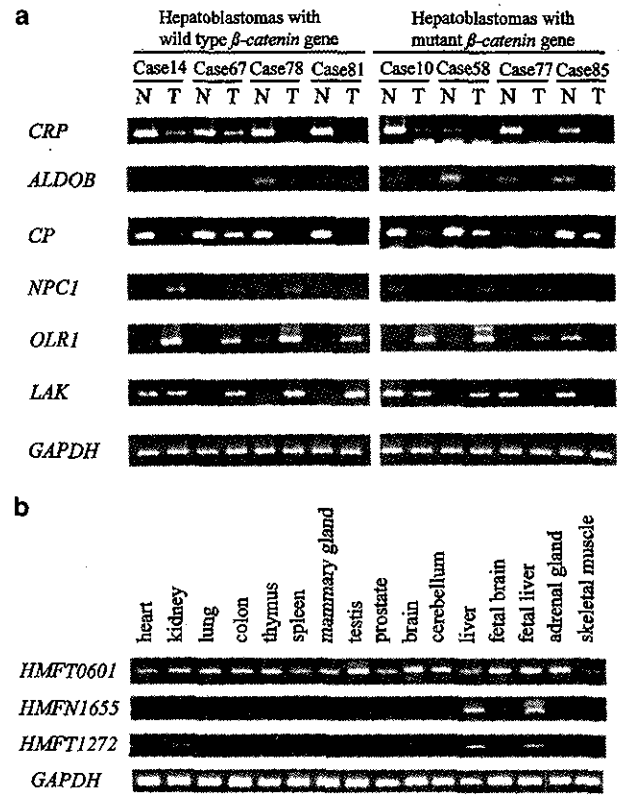

Figure 1 Expression of the representative genes by semi-quantitative RT–PCR. (**a**) Differentially expressed genes between HBLs with or without *β-catenin* mutation and the corresponding normal livers. cDNA was synthesized from RNAs prepared from eight pairs of tumors and their corresponding normal livers, and was used as a PCR template. Amount of cDNAs was normalized to that of *GAPDH*. Four tumors (cases 14, 67, 78, and 81) were with wild-type *β-catenin* gene, while the other four tumors (cases 10, 58, 77, and 85) were with mutant *β-catenin* gene. Gene symbols were shown on the left; *CRP*: C-reactive protein, *ALDOB*: aldolase, *CP*: ceruloplasmin, *NPC1*: Niemann–Pick disease, type C1, *OLR1*: oxidized low-density lipoprotein receptor 1, *LAK*: lymphocyte alpha-kinase. N: normal, T: tumor. (**b**) Semiquantitative RT–PCR of multiple human tissues. *HMFT0601* exhibited ubiquitous expression in all tissues examined, whereas *HMFN1655* and *HMFT1272* showed specific expression in liver and fetal liver

activity, is upregulated in HBLs, suggesting that the IGF axis may be involved in development of the tumor (Gray *et al*., 2000).

Four known genes which were expressed at high levels in HBLs (tumor > normal liver) include GTP-binding

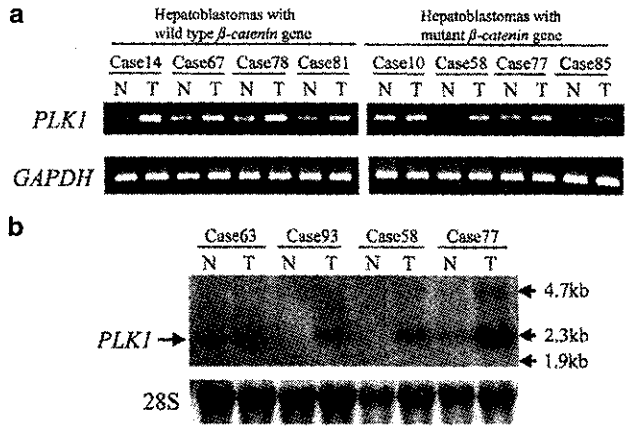

Figure 2 Increased expression of *PLK1* in HBLs. (**a**) Semiquantitative RT–PCR of *PLK1* gene in eight HBL cases. Preferential expression of the *PLK1* was seen in all sample pairs with and without *β-catenin* mutation. (**b**) Northern blot analysis of *PLK1* in primary HBLs, The 28S ribosomal band is shown as a control of each RNA amount

nuclear protein gene *RAN*, *PLK1* onocgene, and two cholesterol metabolism-associated protein genes, *low-density lipoprotein (LDL) receptor 1* and *Niemann-Pick disease type C1 (NPC1)*. The RAN protein is involved in the control of nucleo-cytoplasmic traffic of many nuclear proteins through formation of the transport nuclear pore complex (Ribbeck *et al*., 1998). Nagata *et al*. (2003) also reported that *RAN* is upregulated in HBLs by oligonucleotide DNA array experiment. The LDL receptor 1 binds LDL, a major plasma cholesterol-carrying lipoprotein, and plays an important role in cholesterol homeostasis (Sudhof *et al*., 1987; Goldstein and Brown, 1990; Hamanaka *et al*., 1992). *NPC1* is a causal gene of Niemann–Pick type C disease which is an autosomal recessive lipid storage disorder that affects the viscera and central nervous system (Brady *et al*., 1989). It encodes a protein with sequence similarity to the morphogen receptor 'patched', and to the cholesterol-sensing regions of 3-hydroxy-3-methylglutaryl coenzyme A (HMG-CoA) reductase (Loftus *et al*., 1997) and is involved in the intracellular trafficking of cholesterol. Concerning the differentially expressed genes which contained unknown sequences, those cDNA sequences have been submitted to the public database (Genbank/DDBJ Accession numbers: AB073346-AB073347, AB073382-AB073387, AB073599-AB073614, and AB075869-AB075881). Interestingly, only one known gene, *lymphocyte alpha-kinase (LAK)*, showed distinct expression pattern between HBLs with mutant *β-catenin* and those with wild type *β-catenin* (Figure 1a).

We next examined expression pattern of the novel genes in human multiple tissues by semi-quantitative RT–PCR and found that at least five genes were specifically expressed in the liver (a part of the data is shown in Figure 1b). Since the oncogene *PLK1* (*polo-like kinase-1*) was expressed in HBLs at significantly high levels as compared with the corresponding normal livers, we further examined the role of its expression in HBL.

PLK1 oncogene is overexpressed in HBLs

Recent studies have demonstrated that the preferential expression of *PLK1* mRNA is associated with some cancers including non-small-cell lung cancer (Wolf *et al*., 1997), squamous cell carcinoma of the head and neck (Knecht *et al*., 1999), and esophageal carcinoma (Tokumitsu *et al*., 1999). However, the role of *PLK1* in HBL has never been reported. As indicated by semi-quantitative RT–PCR described above, we found that *PLK1* mRNA expression in HBLs is higher than in normal livers (Figure 2a). Northern blot analysis also confirmed its higher expression in HBLs (Figure 2b). We also performed Southern blot analysis by using the genomic DNAs obtained from primary HBLs and human placenta as a control, and probed with the *PLK1*-specific DNA fragment. However, we failed to find any clue of rearrangements or amplification of the *PLK1* gene locus (data not shown).

To examine the clinical significance of the expression level of *PLK1*, we performed quantitative real-time RT–PCR analysis using 74 primary hepatoblastomas and 29 corresponding normal liver samples (Figure 3a). The average arbitrary values of *PLK1* expression in HBLs and normal livers were 28.9 ± 6.7 and 4.1 ± 0.76, respectively (mean $\pm$ s.e.m., $P < 0.01$). The average values in alive and dead cases were 21.7 ± 5.2 ($n = 61$) and 62.4 ± 28.2 ($n = 13$), respectively ($p = 0.021$). When we compared the expression levels of *PLK1* between 24-paired HBLs and their corresponding normal livers, the former in HBL samples was significantly higher in comparison with the latter ($P < 0.01$) (Figure 3b). We also examined the relationship between the expression levels of *PLK1* and clinicopathological data of HBLs. Statistically significant correlation was observed only between histology and *PLK1* expression ($p = 0.041$). The expression level of *PLK1* in the tumors with poorly differentiated histology was higher than those with the well-differentiated one. The other clinicopathological factors such as age, clinical stage, and *β-catenin* mutation did not show a statistical significance with *PLK1* expression.

To further examine whether the *PLK1* expression was associated with the outcome of the patients with HBL, we performed a Kaplan–Meier analysis (Figure 4). The distinction between high and low levels of *PLK1* expression was based on the median value (low, *PLK1* < 13 d.u.; high, *PLK1* $\geq$ 13 d.u.). Since the overall survivals of 15 out of 74 cases were unknown, 59 cases were applied to the analysis. The 5-year survival rates of the groups with high and low *PLK1* expression were 55.9 and 87.0%, respectively ($P = 0.042$). The univariate analysis showed that both *PLK1* expression ($P = 0.015$) and histology ($P = 0.025$) have a significant prognostic importance (Table 4). The multivariate analysis demonstrated that *PLK1* expression was significantly related to survival, after controlling *β-catenin* mutation, age, stage,

Table 3 The known genes differentially expressed between hepatoblastomas and normal livers

	Gene symbol	*Acc. no*	*Gene name*
Protein synthesis, metabolism, transport			
T>N	RAN	NM_006325	GTP-binding nuclear protein RAN
N>T	LBP	AF105067	Lipopolysaccharide-binding protein
N>T	TDO2	BC005355	Tryptophan 2,3-dioxygenase
N>T	CRP	X56692	C-reactive protein
N>T	GC	NM_000583	Group-specific component
N>T	HP	K01763	Haptoglobin
N>T	HPX	NM_000613	Hemopexin
N>T	SQSTM1	NM_003900	Sequestosome 1
N>T	PHDGH	AF171237	A2-53-73 3-phosphoglycerate dehydrogenase
N>T	PPP1R3C	XM_005398	Protein phosphatase 1, regulatory (inhibitor) subunit 3C
N>T	ITIH4	D38595	Inter-alpha-trypsin inhibitor family heavy chain-related protein
N>T	G1P2	M13755	Interferon-induced 17-kDa/15-kDa protein
Cytokine, growth factor, hormones			
N>T	HABP2	D49742	Hyaluronan binding protein 2
N>T	IGFBP3	NM_000598	Insulin-like growth factor binding protein 3
N>T	GOT1	AF052153	Glutamic-oxaloacetic transaminase 1
Cell signaling			
N>T	CSNK2B	M30448	Casein kinase II, beta polypeptide
N>T	TPD52	NM_005079	Tumor protein D52
cell cycle			
T>N	PLK1	X73458	PLK1
Cell structure, adhesion			
N>T	LRG	AF403428	Leucine-rich alpha-2-glycoprotein
N>T	PGRP-L	AF384856	Peptidoglycan recognition protein L precursor
N>T	CLDN4	NM_001305	Claudin4
N>T	VTN	NM_000638	Vitronection
Organism defense			
N>T	RODH-4	NM_003708	Retinol dehydrogenase 4
N>T	MASP1	AF284421	Mannan-binding lectin serine protease 1
N>T	C4BPA	M31452	Complement component 4 binding protein, alpha
Glycometabolism			
N>T	ADH1B	AF153821	Alcohol dehydrogenase 1B, beta polypeptide
N>T	ALDOB	M15657	Aldolase B
Lipid metabolism			
T>N	NPC1	NM_000271	Niemann–Pick disease, type C1
T>N	OLR1	NM_002543	Oxidized low density lipoprotein (lectin-like) receptor 1
N>T	DGAT2	AF384161	Diacylglycerol acyltransferase
N>T	SCP2	NM_002979	Sterol carrier protein 2
N>T	APOA5	AF202890	Apolipoprotein A-V
N>T	AADAC	L32179	Arylacetamide deacetylase
N>T	SAA4	M81349	Amyloid A protein
Transcription			
N>T	BZW1	NM_014670	Basic leucine zipper and W2 domains 1
N>T	CREB-H	NM_032607	CREB/ATF family transcription factor
RNA biogenesis, metabolism			
N>T	HNRPDL	AB017018	Heterogeneous nuclear ribonucleoprotein D-like
Homeostasis, heat shock protein, metabolic enzymes			
N>T	UGT1A	AF297093	UGT1 gene locus
N>T	ALPL	X14174	Liver-type alkaline phosphatase
N>T	SLC10A1	L21893	Solute carrier family 10
N>T	CES1	AF177775	Carboxylestelase
N>T	AKR1D1	Z28339	Aldo-keto reductase family 1, member D1
N>T	AKR1C2	U05598	Aldo-keto reductase family 1, member C2
N>T	CP	D45045	Ceruloplasmin
Others			
N>T	DGCR6L	NM_033257	DiGeorge syndrome critical region gene 6 like
N>T	A1BG	AF414429	Alpha-1-B glycoprotein

T>N: highly expressed in the tumors as compared to normal livers. N>T: highly expressed in normal livers as compared to the tumors

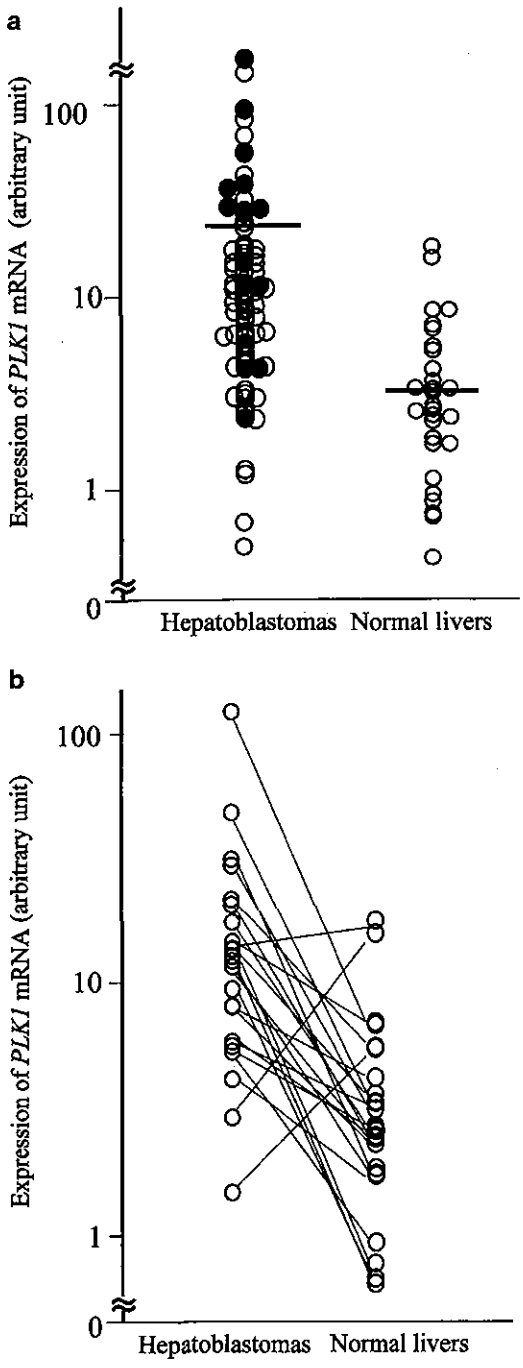

Figure 3 mRNA expression of *PLK1* in HBLs and the corresponding normal livers measured by quantitative real-time RT–PCR. (**a**) The levels of *PLK1* mRNA expression in HBLs and normal livers. The expression levels of *PLK1* were determined by quantitative real-time RT–PCR analysis using 74 HBL tissues and 29 normal livers (see Materials and methods). The *PLK1* expression values were normalized by *GAPDH*. Open and closed circles represent alive and dead, respectively. Since the values of the *PLK1* expression were skewed, a log transformation was used for the expression values. The bars show mean values. (**b**) Correlation of *PLK1* expression between HBL and its corresponding normal liver in 24 paired samples

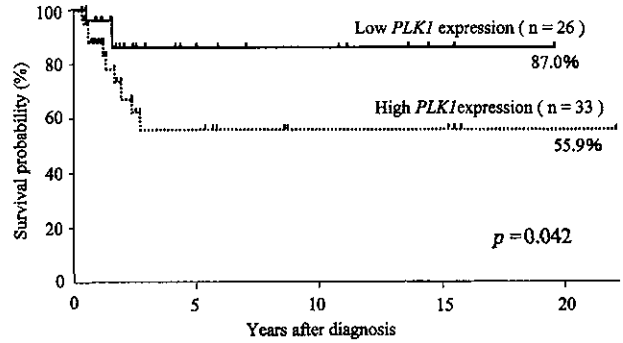

Figure 4 Kaplan–Meier survival curves ($n = 59$) in relation to the expression levels of *PLK1* (median cutoff). The arbitrary median cutoff value was set as 13. The patients with high expression of *PLK1* represented significantly poor prognosis than those with its low expression

Table 4 Univariate Cox regression analysis using *PLK1*(log) and dichotomous factors of *β-catenin* mutation, age, stage, and histology ($n = 59$)

Factor	n	P-*value*	*HR (95% CI)*
PLK1(log)	59	0.015	1.62 (1.10, 2.40)
β-catenin (mutant vs wild type)	58	0.27	1.85 (0.62, .5.56)
Age (>1 vs ≤1 year)	55	0.76	1.22 (0.33, 4.52)
Stage (3, 4 vs 1, 2)	56	0.083	3.81 (0.84, 17.2)
Histology (poorly vs well)	53	0.025	4.48 (1.21, 16.6)

All variables with two categories, except *PLK1*(log); HR = hazard ratio shows the relative of death of first category relative to second; CI = confidence interval

or histology, but marginally related to survival after controlling both histology and stage (Table 5).

Discussion

HBL is one of the embryonal tumors in close relation to the normal as well as abnormal tissue development. To understand the molecular basis of the genesis of HBL, here we randomly cloned a large number of genes expressed in HBLs with or without AFP production and in a non-tumorous infant's liver. Extensive screening for the differentially expressed genes between the tumors and their corresponding normal livers has successfully identified at least 86 genes including 40 with unknown function, which may potentially contribute to develop new therapeutic strategies against HBLs with poor prognosis.

HBL cDNA libraries

We have identified the genes with unknown function in approximately 8% of the total 10431 clones obtained from our oligo-capping cDNA libraries. The comparison of the frequently appeared genes in each libraries shows that expression profile is relatively similar between AFP-positive HBL and the normal part of the infant's liver, whereas it is very different between AFP-positive and AFP-negative tumors, in which many genes